

ANTI-ANGIOGENESIS CHEMOTHERAPY
AGENTS

by

Duygu Çıtak

B.S., Chemistry, Boğaziçi University, 2008

Submitted to the Institute for Graduate Studies in
Science and Engineering in partial fulfillment of
the requirements for the degree of
Master of Science

Graduate Program in Chemistry

Boğaziçi University

2010

To my family

ACKNOWLEDGMENTS

I would like to express my most sincere gratitude to my thesis supervisor Assist. Prof. Rana SANYAL for her endless attention and scientific guidance throughout this study. I appreciate her support and useful comments throughout my laboratory work.

I would extend my thanks to Assoc. Prof. Işıl Aksan Kurnaz for her helpful discussions regarding all my research in this laboratory and for her help during my masters program.

I wish to express my thanks to Prof. İlknur Doğan for her careful and constructive review of the final manuscript and for her care and help during my masters program.

I would like to thank to Burcu Selen Çağlayan and Ayla Türkekul for running a large number of NMR analysis experiments supporting my laboratory work.

I also thank my former and present labmates, Hikmet, Meliha Merve, İpek, Pınar, Tuğba, Damla, İrem, Özgül, Serap, Gülen, Nergiz, Merve, Sebla and my friends Dilan, Mine, Esin, Pelin, Tuna and Burak for their enjoyable company and friendship. I would like to thank all my friends and all the members of the faculty in the Chemistry Department.

Finally, my deepest thanks go to my whole family for their endless love, support and encouragement throughout these years.

This research has been supported by Boğaziçi University BAP 09S107 and TÜBİTAK 107T623.

LIST OF SYMBOLS/ ABBREVIATIONS

<i>J</i>	Coupling constant
ν	Frequency
ACN	Acetonitrile
CDCl ₃	Deuterated chloroform
CH ₂ Cl ₂	Dichloromethane
DCC	<u>N,N'-Diisopropylcarbodiimide</u>
DMAP	4-Dimethylaminopyridine
EtOAc	Ethyl Acetate
EtOH	Ethanol
FT-IR	Fourier Transform Infrared
HPLC	High Performance Liquid Chromatography
MeOH	Methanol
MHz	Mega hertz
NMR	Nuclear Magnetic Resonance
Prep-HPLC	Preparative High Performance Liquid Chromatography
TEA	Triethylamine
THF	Tetrahydrofuran
TLC	Thin Layer Chromatography
UV	Ultraviolet

ABSTRACT

ANTI-ANGIOGENESIS CHEMOTHERAPY AGENTS

Angiogenesis can be explained as the growth of new blood vessels from pre-existing vasculature. It has an important and vital role in growth and development, as well as in wound healing. Anti-angiogenic substances suppress the growth of new blood vessels so prevent nutrients and oxygen needed for the growing of tumor cells. It is proposed that tumor angiogenesis could serve as a potential target for anticancer therapy.

Combretastatin (CA-4) is an anti-angiogenesis agent that inhibits the tubulin polymerization. CA-4 exhibits anti-tumor effects through the well-organized therapeutic mechanism of tumor blood supply disabling. By affecting selectively and blocking tumor vasculature, CA-4 reduces the blood supply needed for tumor growth and survival. As a result of oxygen poverty and build-up of tumor metabolic by-products causes the death of the cancer cells within the central core of the tumor. In this thesis, covalent modification of CA-4 has been investigated. Variety of CA-4 analogs which involved blocking the free alcohol group has been synthesized.

ÖZET

ANTI-ANJİYOGENEZ KEMOTERAPİ ETKENLERİ

Anjiyogenez önceden va rolan kan damarlarından yeni damarların büyümesi olarak açıklanabilir. Anjiyogenezin büyüme ve gelişimde hayati bir role sahip olmasının yanı sıra yara iyileşmesinde de önemli bir faktördür. Anti-anjiyogenik maddeler yeni kan damarlarının büyümesini önler böylece, tümör hücrelerinin büyümesi için gerekli olan besin ve oksijen ihtiyacını engeller. Tümör anjiyogenezi, anti-kanser tedavisi için potansiyel çözüm olarak görülmektedir.

Combretastatin (CA-4) tubulin polimerizasyonunu engelleyen bir anti-anjiyogenik bir etkidir. CA-4, tümör damarlarını bloke eden iyi organize edilmiş bir mekanizma yoluyla, anti-tümör etkiler sergilemektedir. Tümör damarlarını seçici olarak etkileyerek ve bloke ederek, tümörlerin büyümesi ve hayatta kalması için gerekli olan kan ihtiyacını azaltmaktadır. Oksijen yetersizliği ve tümör mekanizmasında oluşan yan ürünler, tümör çekirdeğinde kanser hücrelerinin ölümüyle sonuçlanmaktadır. Bu tezde, CA-4 molekülünün kovalent bağ ile modifikasyonu incelenmiştir. Serbest alkol grubu engelleyen çeşitli CA-4 analogları sentezlenmiştir.

TABLE OF CONTENTS

ACKNOWLEDGMENTS	iv
LIST OF SYMBOLS/ ABBREVIATIONS	v
ABSTRACT	vi
ÖZET	vii
LIST OF FIGURES	x
LIST OF TABLES	xiii
1. INTRODUCTION	1
1.1. Cancer	1
1.1.1. Cancer Treatment	3
1.2. Angiogenesis	4
1.2.1. Angiogenesis Inhibitors	6
1.3. Combretastatin	8
1.3.1 Combretastatin A-4 phosphate	12
1.4. Polymer Therapeutics	14
2. AIM OF THE STUDY	19
3. RESULTS AND DISCUSSION	20
3.1. Synthesis of Cis-Combretastatin A-4	20
3.2. Funtionalization of Cis-Combretastatin A-4	23
4. EXPERIMENTAL	34
4.1. Materials and Methods	34
4.2. Synthesis	34
4.2.1. Synthesis of Cis Combretastatin A-4	34
4.2.1.1. Synthesis of E-2-(3',4',5'-Trimethoxyphenyl)-3-(3'-hydroxy-4'-methoxyphenyl) prop-2-enoic acid	34
4.2.1.2. Synthesis of Combretastatin A4 by Decarboxylation of Cinnamic Acid	35
4.2.2. Synthesis of (Z)-5-(3,4,5-trimethoxystyryl)-2-methoxyphenyl-2-aminoacetate via deprotection of t-BOC derivative reaction	36
4.2.2.1. Synthesis of (Z)-5-(3,4,5-trimethoxystyryl)-2-methoxyphenyl-2-(tert- butoxycarbonyl) acetate	36
4.2.2.2. Synthesis of (Z)-5-(3,4,5-trimethoxystyryl)-2-methoxyphenyl-2-	

aminoacetate 4	36
4.2.3. Synthesis of (Z)-5-(3,4,5-trimethoxystyryl)-2-methoxyphenyl-2-aminoacetate via Gabriel reaction	37
4.2.3.1 Synthesis of (Z)-5-(3,4,5-trimethoxystyryl)-2-methoxyphenyl-2-bromoacetate.....	37
4.2.3.2. Synthesis of (Z)-5-(3,4,5-trimethoxystyryl)-2-methoxyphenyl-2-(1,3-dioxoisindolin-2-yl)acetate	37
4.2.3.3. Synthesis of (Z)-5-(3,4,5-trimethoxystyryl)-2-methoxyphenyl-2-aminoacetate	38
4.2.4. Synthesis of (Z)-5-(3,4,5-trimethoxystyryl)-2-methoxyphenyl-2-aminoacetate via Staudinger reaction	39
4.2.4.1. Synthesis of (Z)-5-(3,4,5-trimethoxystyryl)-2-methoxyphenyl-2-azidoacetate	39
4.2.4.2. Synthesis of (Z)-5-(3,4,5-trimethoxystyryl)-2-methoxyphenyl-2-aminoacetate	39
4.2.5. Synthesis of (Z)-5-(3,4,5-trimethoxystyryl)-2-methoxyphenyl-4-aminobutanoate via Staudinger reaction	40
4.2.5.1 Synthesis of (Z)-5-(3,4,5-trimethoxystyryl)-2-methoxyphenyl-4-azidobutanoate	40
4.2.5.2. Synthesis of (Z)-5-(3,4,5-trimethoxystyryl)-2-methoxyphenyl-4-aminobutanoate.....	40
APPENDIX ..	42
REFERENCES	54

LIST OF FIGURES

Figure 1.1.	Pathway to cancer	1
Figure 1.2.	An image of tumor <i>in vivo</i>	2
Figure 1.3.	Common diseases and causes of death	3
Figure 1.4.	Vascular endothelial cells	5
Figure 1.5.	Schematic representations of VEGF family ligands and their receptors.	6
Figure 1.6.	Angiogenesis in tumor cells	7
Figure 1.7.	African willow trees <i>Combretum caffrum</i>	9
Figure 1.8.	Combretastatin A-4	9
Figure 1.9.	Selected analogues of CA-4 modified on the aromatic rings A and B ...	10
Figure 1.10.	Dose effect of CA-4 to vascular volume of mice	11
Figure 1.11.	Effect of CA-4 in chromatin condensation to HUVECs	12
Figure 1.12.	Prodrug of CA-4 molecule	12
Figure 1.13.	Effect of CA-4P to tumor tissue	14
Figure 1.14.	Schematic representation of polymer-drug conjugate	15
Figure 1.15.	Schematic representation of EPR effect	16
Figure 1.16.	Structure of PPX	17
Figure 1.17.	Plasma concentration of taxane	18
Figure 1.18.	Tumor concentration of taxane	18
Figure 2.1.	Schematic representation of functionalized drug-macromolecule conjugate	19
Figure 3.1.	Schematic representation of the synthesis of CA-4 analogues	20
Figure 3.2.	Synthesis of propenoic acid intermediate 13	21
Figure 3.3.	HPLC spectrum of propenoic acid 13	21

Figure 3.4.	^1H NMR of propenoic acid 13	22
Figure 3.5.	^1H NMR spectrum of CA-4 1	22
Figure 3.6.	HPLC spectrum of CA-4 1	23
Figure 3.7.	Schematic representation of drug- macromolecule conjugation	23
Figure 3.8.	Reaction of CA-4 with BOC-Gly-OH 3	24
Figure 3.9.	^1H NMR spectrum of the molecule 3	24
Figure 3.10.	HPLC spectrum of the molecule 3	25
Figure 3.11.	Deprotection reaction of amine 4	25
Figure 3.12.	FTIR spectrum of amine-terminated CA-4 molecule 4.....	26
Figure 3.13.	HPLC of molecule 4	26
Figure 3.14.	Gabriel synthesis.....	27
Figure 3.15.	^1H NMR of molecule 6.....	27
Figure 3.16.	HPLC of molecule 6	28
Figure 3.17.	^1H NMR of the molecule 7	28
Figure 3.18.	HPLC of the molecule 7	29
Figure 3.19.	Synthesis of azide-terminated CA-4 molecule	30
Figure 3.20.	FTIR spectrum of azide-terminated CA-4 molecule 8	30
Figure 3.21.	Staudinger reduction.....	30
Figure 3.22.	Synthesis of the molecule 10.....	31
Figure 3.23.	^1H NMR of the product 10	31
Figure 3.24.	HPLC of the product 10	32
Figure 3.25.	Reduction of the molecule 10.....	32
Figure 4.1.	Perkin Condensation of 3,4,5-Trimethoxyphenylacetic Acid 11 and 3-Hydroxy-4 methoxybenzaldehyde 12	35
Figure 4.2.	Synthesis of Combretastatin A-4 1 by Decarboxylation of Cinnamic	

Acid	35
Figure 4.3. Synthesis of the molecule 3	36
Figure 4.4. Synthesis of molecule 4 via deprotection of t-boc derivative.....	37
Figure 4.5. Synthesis of molecule 6.....	37
Figure 4.6. Synthesis of molecule 7.....	38
Figure 4.7. Gabriel Synthesis of molecule 4.....	38
Figure 4.8. Synthesis of molecule 8.....	39
Figure 4.9. Synthesis of molecule 4.....	40
Figure 4.10. Synthesis of molecule 10.....	40
Figure 4.11. Synthesis of molecule 14.....	41
Figure A.1. ¹ H NMR of propenoic acid 13.....	43
Figure A.2. ¹ H NMR of CA-4 1.....	44
Figure A.3. ¹ H NMR of the molecule 3	45
Figure A.4. ¹ H NMR of the molecule 4.....	46
Figure A.5. ¹ H NMR of the molecule 6.....	47
Figure A.6. ¹ H NMR of the molecule 7	48
Figure A.7. ¹ H NMR of the molecule 10.....	49
Figure A.8. IR spectrum CA-4 1.....	50
Figure A.9. IR spectrum of molecule 3.....	51
Figure A.10. IR spectrum of the molecule 4.....	52
Figure A.11. IR spectrum of the molecule 8.....	53

LIST OF TABLES

Table 1.1.	Anti-angiogenic therapy: compounds and their mechanism of action	8
Table 1.2.	Pharmacokinetic Properties of PPX and Standard Paclitaxel.....	17
Table 3.1.	IC50 values of CA-4 analogs (nM).....	33

1. INTRODUCTION

1.1. Cancer

Malignant neoplasm, with its most common name “cancer”, is not only one disease but class of diseases with more than 100 different types, in which a group of cells show uncontrolled growth. These abnormal cells differ from the normal cells that they can also invade to adjacent tissues (invasion) and sometimes diffuse to the other parts of the body through lymph or blood (metastasis).

Cells proceed to metastasis cancer after several stages. Regulations can increase the number of cells (proliferation), block differentiation into specialized cells, prevent cell death (apoptosis) that can eliminate cancer cells, activate the blood supply required to continue cell growth (angiogenesis), and permit movement out of the tumor (metastasis) [1]. These events can occur in different orders thereby different intermediate stages will be observed but the major three-step pathway is shown in figure 1.1.[2].

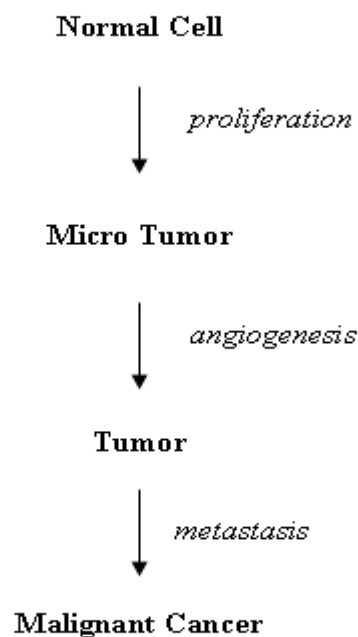


Figure 1.1. Pathway to cancer [2]

Cancer cells damage to DNA that exists in every cell and controls all its actions. In a normal cell, if DNA is damaged, it can be repaired or it is terminated with the death of the cell. However in cancer cells, DNA is not repaired, even, new abnormal cells are formed.

Damaged DNA can be inherited or it can be formed by mistakes during the reproduction of normal cells. Sometimes it can occur from something obvious like tobacco, sunlight, certain chemicals or radiation but often the cause is not clear.

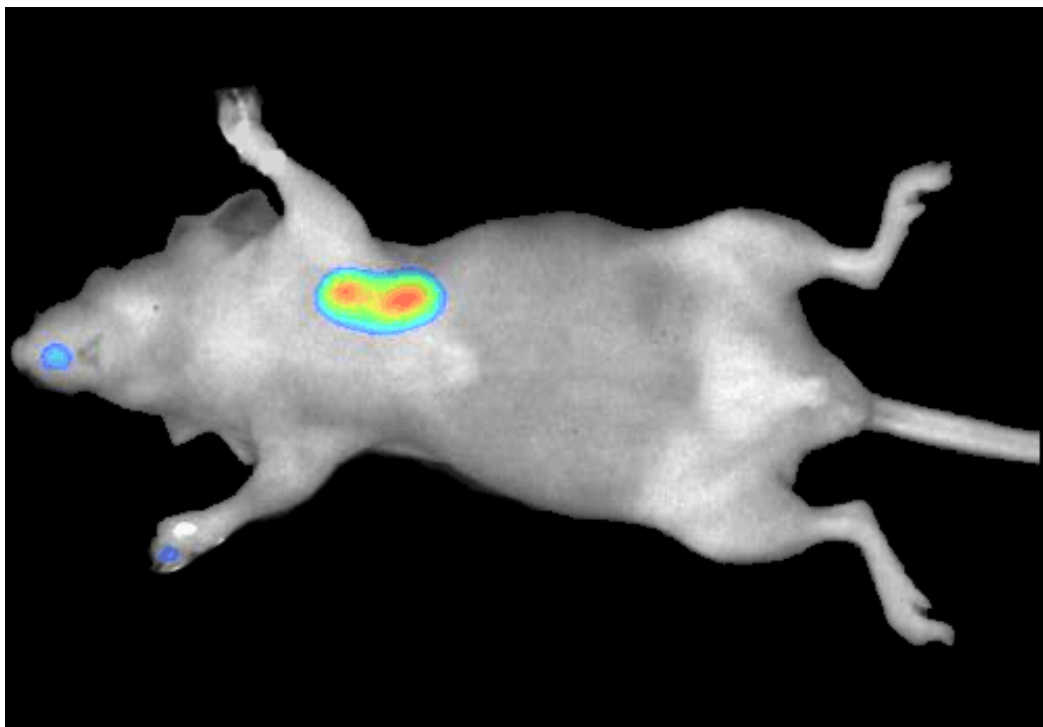


Figure 1.2. An image of tumor *in vivo* [3]

Most of the cancer types form a tumor [Figure 1.2] [3]. Some types, like leukemia do not form tumors. These cancer cells include the blood and blood-forming organs and accumulate through other tissues where they grow.

Cancer is the second leading cause of death all around the world [Figure 1.3] [4]. The World Health Organization explains that 7.6 million people died of cancer in 2005 and 84 million people will die in the next 10 years if action is not taken [5]. About 70% of all cancer deaths take place in low and middle-income countries, because of the lack of resources for prevention, diagnosis and treatment.

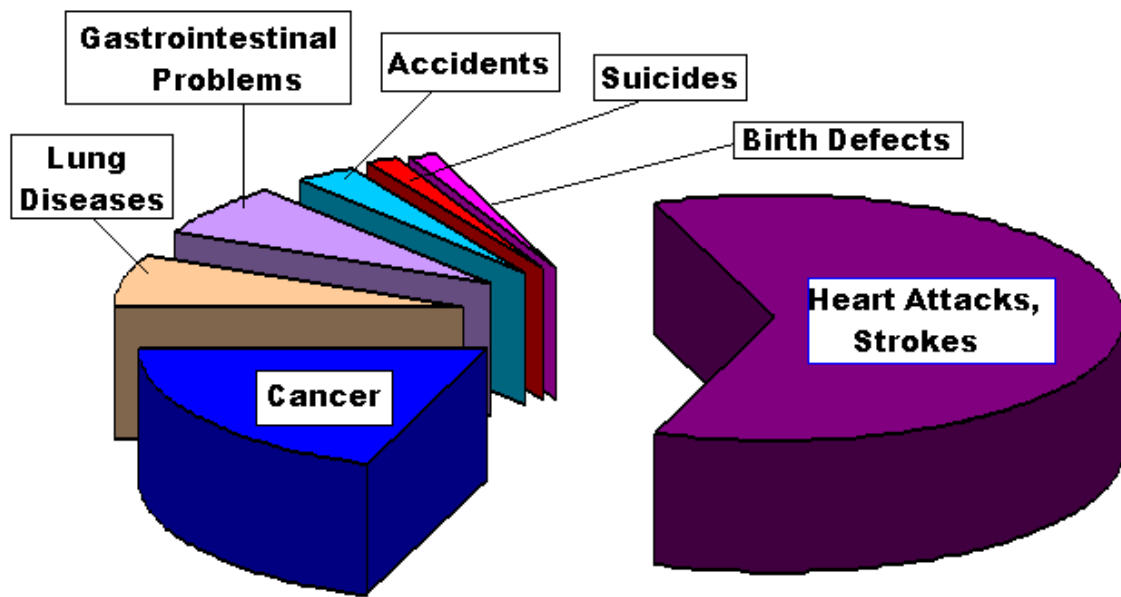


Figure 1.3. Common diseases and causes of death [4]

1.1.1 Cancer Treatment

Treatment of the disease intends to cure, prolong life, and provide a qualified life to the patients for the rest of their lives. Most of the time efficiency of treatment is based on the early detection of cancer.

After diagnosis of the disease, depending on the type, grade and location, most cancers can be treated by surgery, chemotherapy, radiation therapy, immunotherapy or monoclonal antibody therapy and some can be cured.

Chemotherapy is the treatment of cancer with anticancer drugs that can destroy cancer cells. As cancer is a class of diseases, there will hardly ever be a single cure. And it is obvious that cancer chemotherapy is a very difficult process. Chemotherapy acts with chemicals acting by killing rapid dividing cells which is one of the main properties of tumor cells. However because of the biodistribution throughout the body, that also means that chemotherapy harms all the cells that divide rapidly under normal circumstances, like the cells in the hair follicles, bone marrow and digestive tract. Also as a result of biodistribution, a large total dose of chemotherapy agent is required to accumulate high concentrations in a tumor cell. That is the main reason of the most common side effects of chemotherapy.

In recent years, researchers have been studying on newer therapy that anticancer drugs act directly against abnormal proteins in cancer cells which is called targeted therapy.

Targeted therapy prevents the growth of cancer cells with specific targeted molecules rather than by simply interfering with rapidly dividing cells. The purpose of the treatment is to cure the disease without giving any damage to the other parts of the body. Targeted therapy drugs can act specifically on detectable abnormalities in certain tumors thus the damage to the normal cells will be inhibited.

Although the studies on cancer therapies increase every day, about half of cancer patients are not cured by the known treatments. Even, some of the patients are affected more by the side-effects of the cytotoxic chemotherapy agents. 600 patients who died within 30 days of treatment, 27% had their deaths hastened or caused by chemotherapy [6].

1.2. Angiogenesis

Angiogenesis can be defined as the growth of new blood vessels from pre-existing microvasculature [7]. It has an important and vital role in growth and development, as well as in wound healing.

The interior surface of blood vessels is formed by vascular endothelial cells which reduce turbulence of the flow of blood [Figure 1.4] [8]. Endothelial cells are needed in many activities of vascular biology, including the control of blood pressure, blood clotting (thrombosis & fibrinolysis) and formation of new blood vessels. These cells are divided seldom, about once every 3 years on average. However, when needed, angiogenesis can stimulate them to divide.

Angiogenesis is regulated by both pro- and anti-angiogenic regulators [9]. Normally, growth is blocked by the predominant inhibitors. However, when the requirement for new blood vessels arises, number of pro-angiogenic activators increases and inhibitors decrease, stimulating the growth and division of vascular endothelial cells and as a result, the formation of new blood vessels.

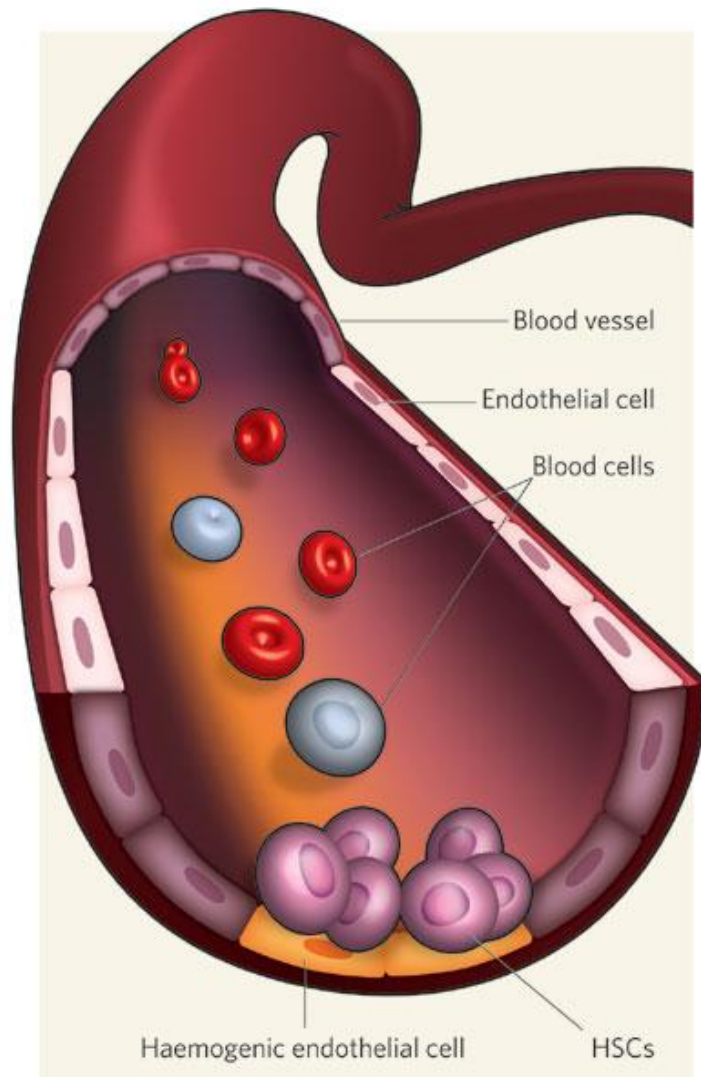


Figure 1.4 Vascular endothelial cells [8]

Vascular endothelial growth factor (VEGF), one of the pro-angiogenic regulators, has an important role at all stages of angiogenesis for blood vessel formation during embryonic development, in wound healing and in maintaining vessel homeostasis in adult organisms. VEGF is an activator of endothelial cell proliferation and mobility [10]. All members of the VEGF family stimulate cellular responses by binding to tyrosine kinase receptors (the VEGFRs) on the cell surface, provoking them to dimerize and become activated and as a result causing angiogenesis [Figure 1. 5] [11].

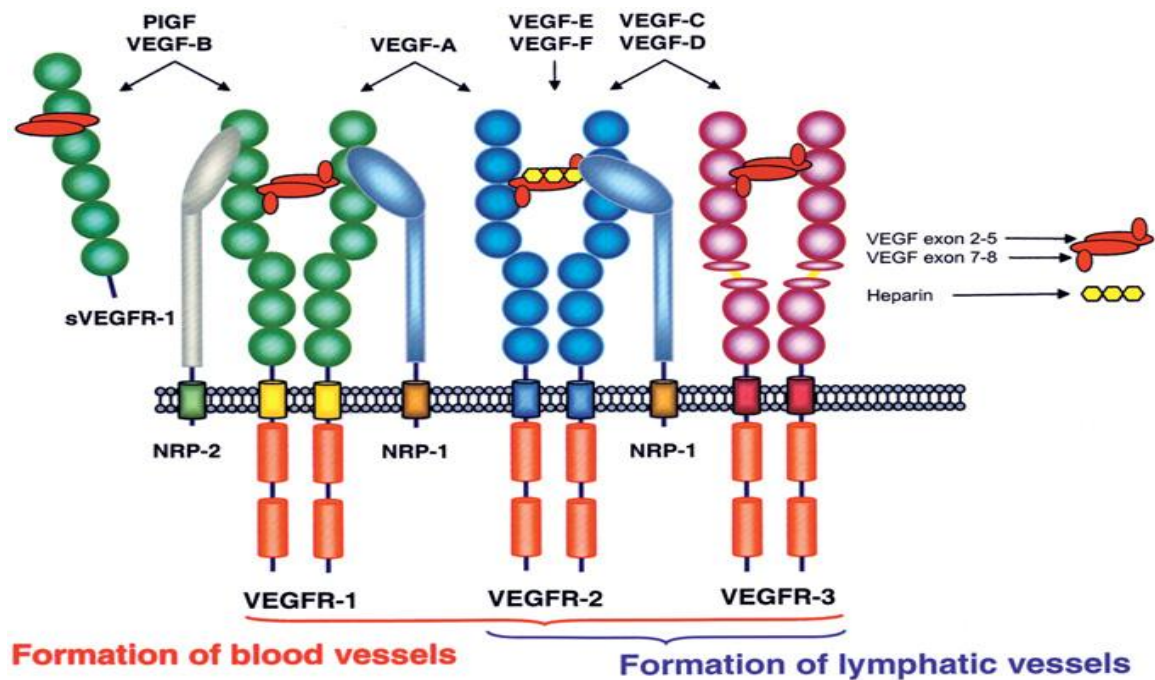


Figure 1.5 Schematic representations of VEGF family ligands and their receptors [11]

1.2.1. Angiogenesis Inhibitors

Tumor angiogenesis is the proliferation of a network of blood vessels that penetrates into cancerous growths, supplying nutrients and oxygen and removing waste products [12]. Cancerous tumor cells release molecules that send signals to normal host tissue around them to activate certain genes for stimulation of the growth of new blood vessels.

Before the 1960s, it was believed that the blood supply reached tumors because of the dilation of pre-existing blood vessels. But in recent years, it is shown that for the growth and spread of cancerous tumors, angiogenesis is a must [Figure 1.6] [13]. Benefiting from that idea, it is proposed that tumor angiogenesis could serve as a potential target for anticancer therapy.

Anti-angiogenic substances inhibit the growth of new blood vessels. As angiogenesis supplies nutrients and oxygen needed for the growing of tumor cells, suppressing the building of blood vessels by anti-angiogenic agents prevents cancer from growing indefinitely.

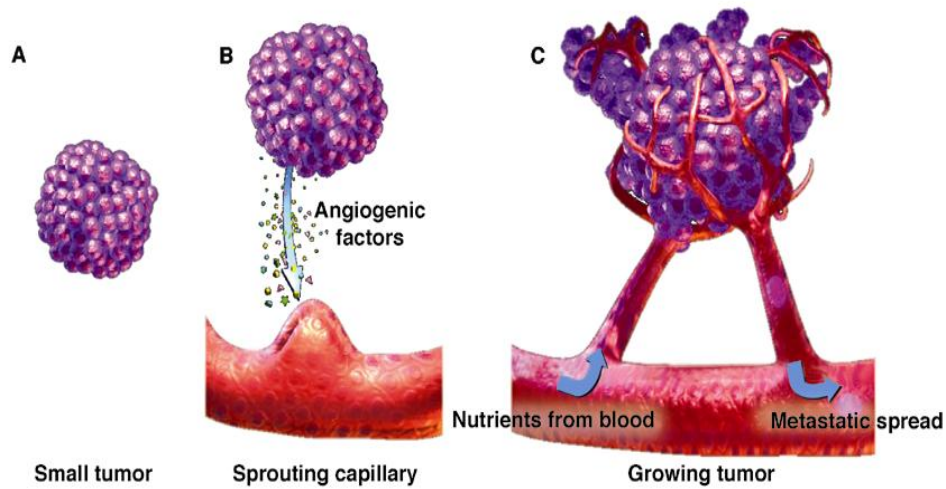


Figure 1.6 Angiogenesis in tumor cells [13]

Angiogenesis inhibitors were thought to have potential as a "silver bullet" treatment applicable to many types of cancer. In contradistinction to traditional chemotherapy, anti angiogenesis agents do not attack cancer cells directly but target blood vessels specifically to prevent the growth of new tumors.

Vascular endothelial growth factor (VEGF), released by cancerous cells attaches to a receptor (called the VEGF receptor, or VEGFR) on the surface of surrounding endothelial cells. This action signals the cells' control centers and the growing and forming new blood vessels starts. To specifically inhibit the formation of new blood vessels, many molecules related with vascular endothelial growth factors (VEGF)-based and non-VEGF-based anti-angiogenic therapies are being evaluated in clinical trials [Table 1] [14]. For example Bevacizumab (Avastin[®]), a humanized monoclonal antibody, is the first U.S. Food and Drug Administration (FDA) approved drug which binds VEGF to inhibit its binding to the receptors to stimulate angiogenesis [15].

Angiogenesis inhibitors are rarely toxic to most healthy cells so do not cause bone marrow suppression, gastrointestinal symptoms, or hair loss. When traditional chemotherapy drugs are used for a long period of time, tumors develop a resistance to these agents. Luckily, such a resistance do not observed with angiogenesis inhibitors.

Table 1.1 Anti-angiogenic therapy: compounds and their mechanism of action [14]

Compound	Mechanism of action
Inhibitors of ECM remodeling	
Batimastat, marimastat, AG3340, Neovastat, PEX, TIMP-1, -2, -3, -4 PAI-1, -2, uPA Ab, uPAR Ab, Amiloride Minocycline, tetracyclines, cartilage-derived TIMP	MMP inhibitors, block endothelial and tumor cell invasion uPA inhibitors, block ECM breakdown Collagenase inhibitors, disrupt collagen synthesis and deposition
Inhibitors of adhesion molecules	
$\alpha_v\beta_3$ Ab: LM609 and Vitaxin, RGD containing peptides, $\alpha_v\beta_3$ Ab Benzodiazapine derivatives	Block EC adhesion, induce EC apoptosis Antagonist of $\alpha_v\beta_3$
Inhibitors of activated endothelial cells	
Endogenous inhibitors: endostatin, angiostatin, aaAT IFN- α , IFN- γ , IL-12, nitric oxide synthase inhibitors, TSP-1 TNP-470, Combretastatin A-4 Thalidomide Linomide	Block EC proliferation, induce EC apoptosis, inhibit angiogenic switch Block EC migration and/or proliferation Block EC proliferation Inhibits angiogenesis <i>in vivo</i> Inhibits EC migration
Inhibitors of angiogenic mediators or their receptors	
IFN- α , PF-4, prolactin fragment Suramin and analogues	Inhibit FGF-2, inhibit FGF-2-induced EC proliferation Bind to various growth factors, including FGF-2, VEGF, PDGF, inhibit EC migration and proliferation
PPS, distamycin A analogues, FGF-2 Ab, antisense-FGF-2 Protamine	Inhibit FGF-2 activity Binds heparin, inhibits EC migration and proliferation
SU5416, soluble Flt-1, dominant-negative Flk-1, VEGF receptor ribosymes, VEGF Ab Aspirin, NS-398 6AT, 6A5BU, 7-DX	Block VEGF activity COX inhibitors TP antagonists
Inhibitors of EC intracellular signaling	
Genistein Lavendustin A Ang-2	Tyrosine kinase inhibitor, blocks uPA, EC migration and proliferation Selective inhibitor of protein tyrosine kinase Inhibits Tie-2

The limitations and the drawbacks of the therapy are due to being administered over a long period. As angiogenesis is needed in wound healing and in reproduction, long-term treatment with anti-angiogenic agents could cause problems with bleeding, blood clotting and heart function.

In addition, combination of anti-angiogenic therapy with some chemotherapy or radiation therapy will be more effective.

1.3. Combretastatin

Combretastatins are natural products derived from the African willow tree *Combretum caffrum* [16] [Figure 1.7] [17]. They are hydroxylated derivatives of stilbene that is a hydrocarbon containing an ethene double bond substituted with a phenyl group on both carbon atoms of the double bond.



Figure 1.7 African willow trees *Combretum caffrum* [17]

Generally, three characteristics are common in all molecules that are the members of the combretastatin family: a trimethoxy "A"-ring, a "B"-ring with substituents often at C3' and C4', and an ethene bridge between the rings which is necessary for structural rigidity [Figure 1.8]. Molecules with C3' amino and hydroxyl substituents are very active, and C4' hydroxyl or methoxy substituents make molecules cytotoxic.

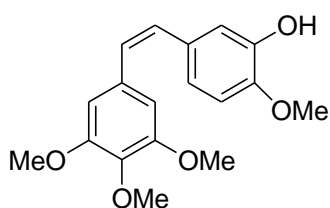


Figure 1.8 Combretastatin A-4

Members of the combretastatin family show varying ability to cause vascular disruption in tumors. Vascular Disrupting Agents (VDAs) are related to anti-angiogenesis but cover a different approach. Instead of inhibiting the formation of new blood vessels, VDAs destroy the existing vasculature of tumors by binding to tubulin, which is a protein found in the cells lining blood vessels. As normal blood vessels have a well-organized scaffolding system, VDAs effect abnormal cells such as tumor cells.

Combretastatin inhibits the tubulin polymerization and thus, prevents production of microtubules of cancer cells as a result of attaching to the β -subunit of tubulin at what is called the colchicine site.

Novel stilbenoid compounds can be easily synthesized. Thus, Up to now, researchers have prepared and described hundreds of combretastatin derivatives with different anti-angiogenic activity and cytotoxicity [Figure 1.9] [18].

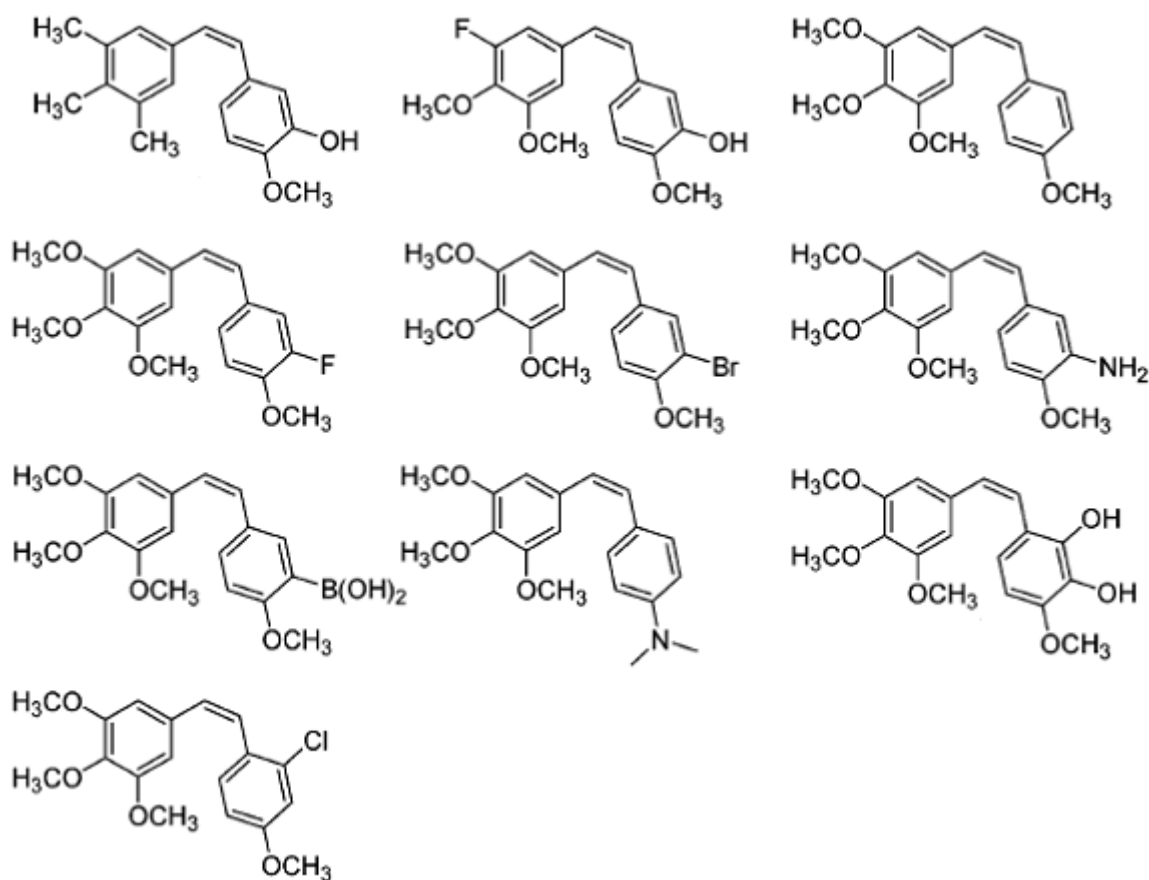


Figure 1.9 Selected analogues of CA-4 modified on the aromatic rings A and B [18]

Inside the Combretastatin family, tubulin-binding drug Combretastatin A-4 (CA-4) exhibits the most active properties in regards to both tubulin binding ability and cytotoxicity despite its low molecular weight and simple molecular structure [19]. Lots of studies have been done to observe the pharmacokinetic properties of CA-4. Figure 1.10 shows the results of studies done with CA-4 to see the dose effect of the molecule to vascular volume of mice. Results are obtained six hours after i.p. administration of CA-4 (25 or 100 mg/kg). Data are

expressed as percentage vascular shutdown relative to the mean vascular volume of untreated tumors and are means for 5 to 13 tumors. At the lower dose, combretastatin A-4 reduced functional vascular volume in the tumor mass by ~30%. At the higher dose, the drug induced essentially complete vascular shutdown [20].

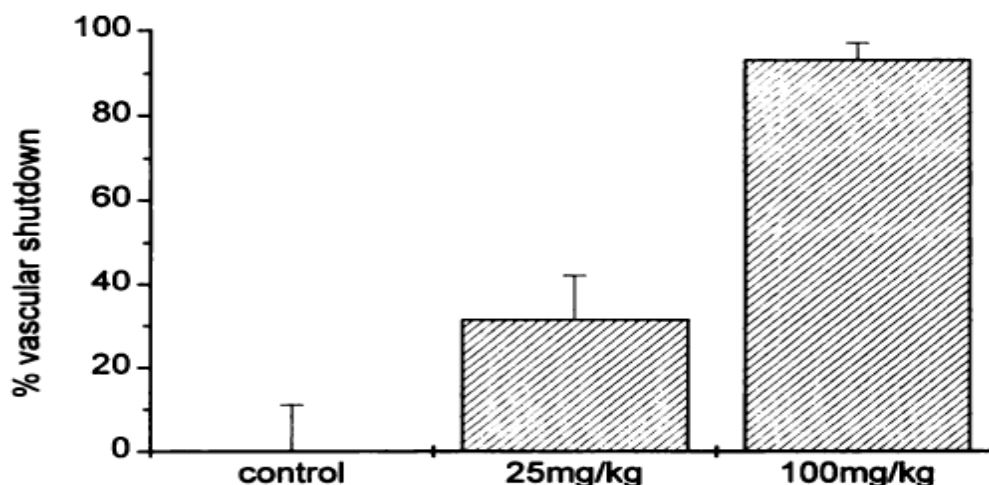


Figure 1.10 Dose effect of CA-4 to vascular volume of mice [20]

Combretastatin A-4 also affects morphology characteristic of apoptosis, the death of cells which occurs as a normal part of an organism's development. To see the effects of Combretastatin A-4 on apoptosis, HUVECs are incubated for 24 hours in the absence of drug and in its presence (0.1 mM) for 6, 16 and 24 hours. The studies done by using Hoechst 33258 staining and fluorescence microscopy reveal that 15% of HUVECs treated with combretastatin A-4 for 24 h exert chromatin condensation and so, programmed cell death, compared with only ~1% of cells incubated in the absence of drug [Figure 1.11] [20].

It is mentioned that CA-4 is a strong tubulin inhibitor. However due to its poor solubility in water, a more soluble pro-drug, CA-4 phosphate (CA-4P), has been developed as the selected lead for in vivo and in human studies.

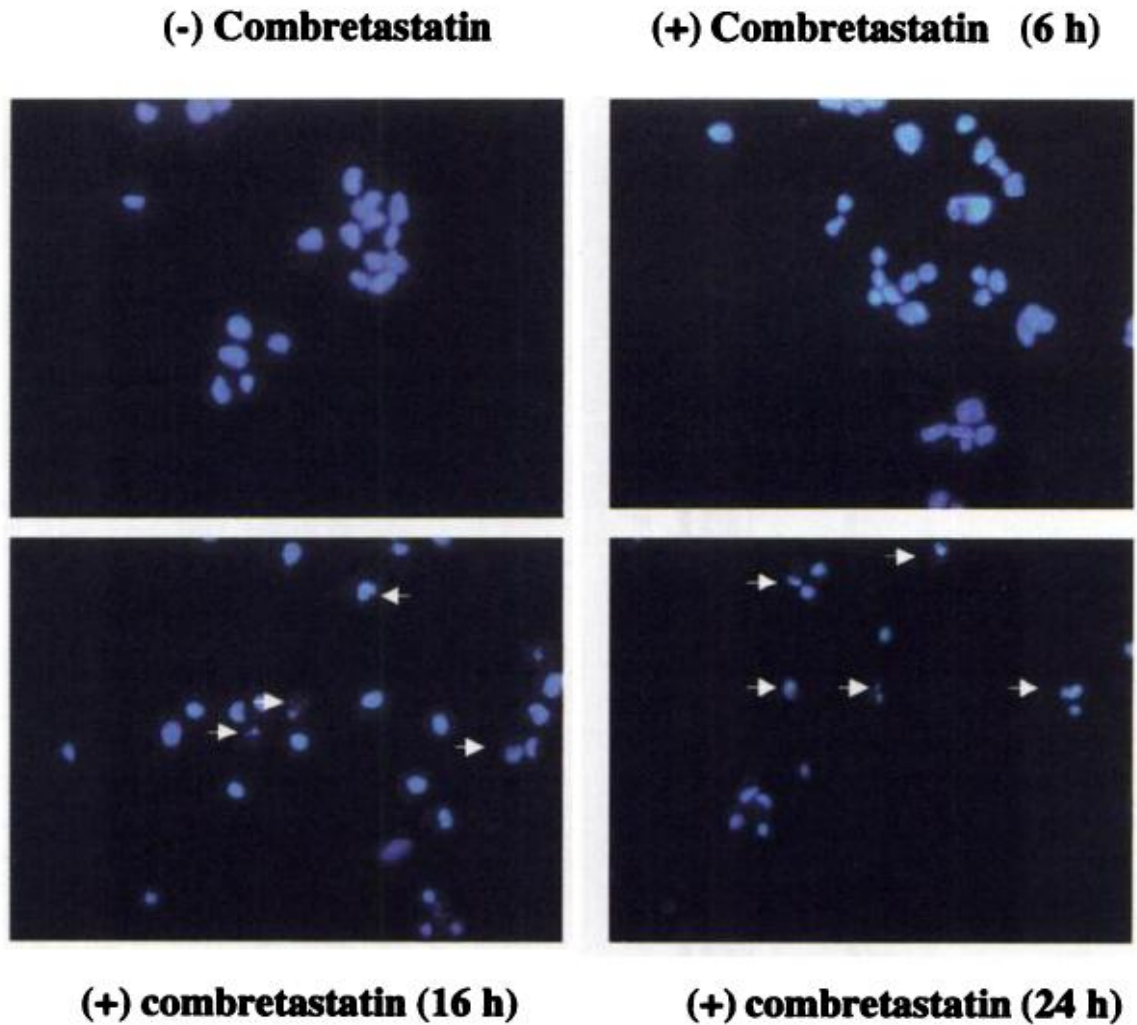


Figure 1.11 Effect of CA-4 in chromatin condensation to HUVECs [20]

1.3.1. Combretastatin A-4 phosphate

Combretastatin A-4 phosphate (CA-4P) is a prodrug with a brand name ZYBRESTAT [Figure 1.12]. After administration, it is dephosphorylated to its active molecule combretastatin A-4, which enters the endothelial cells that line the blood vessels [21].

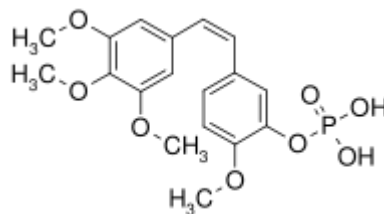


Figure 1.12 Prodrug of CA-4 molecule

CA-4P exhibits anti-tumor effects through the well-organized therapeutic mechanism of tumor blood supply disabling. By affecting selectively and blocking tumor vasculature, CA-4P reduces the blood supply needed for tumor growth and survival. As a result of oxygen poverty and build-up of tumor metabolic by-products causes the death of the cancer cells with in the central core of the tumor.

CA-4P is in phase III clinical trials started in July 2007 by the pharmaceutical company OXiGENE. 180-patient trials have been initiated for CA-4-P in combination with carboplatin for the treatment of anaplastic thyroid cancer, a highly lethal and aggressive form of cancer for which there is currently no fully FDA approved treatment. In clinical studies, CA-4P has exhibited promising results:

- In phase I studies CA-4P indicates significant ability to reduce tumor blood-flow.
- In phase II trials median survival time and one-year survival rate of patients with advanced, relapsed anaplastic thyroid cancer exceed survival statistics of similar patients reported in clinical literature.
- The side effects usually observed when chemotherapy is performed, such as bone marrow toxicity and alopecia, appear to be absent or mild.
- In preclinical studies, synergistic or additive effects are demonstrated when incorporated in various combination regimens with the other treatments [22].

ZYBRESTAT is the first vascular disrupting agent used together with an angiogenesis-inhibiting drug (AVASTIN®) and tested in humans. This study is investigated in a treatment of a model of renal cell carcinoma. It is observed that CA-4P-Avastin combination shows an important improvement in tumor response [Figure 1.13] [23]. The plausible explanation of these results is that while CA-4P reduces the viable tumor mass, Avastin diminishes the tumor growth.

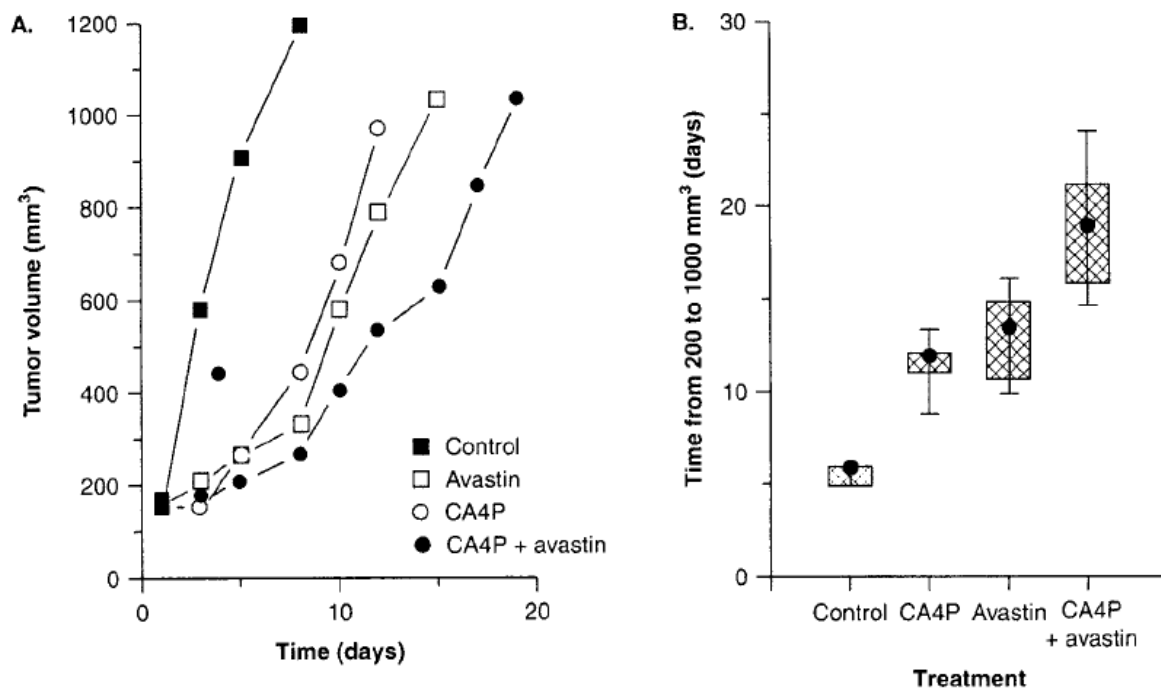


Figure 1.13 Effect of CA-4P to tumor tissue [23]

1.4. Polymer Therapeutics

Polymer Therapeutics is an umbrella used to describe polymeric drugs, polymer-drug conjugates, polymer-protein conjugates and polymeric micelles [24].

Chemotherapy agents widely used in clinical to date are low molecular weight compounds that lead to a short half-life in the blood stream and a high overall clearance rate. They disperse into healthy tissues rapidly and are distributed within the body. As a result, relatively small amounts of the drug reach to the malignant cells, and treatment causes many side effects which are dose-limiting and thus effective treatment is limited.

Luckily, most chemotherapy agents have improvable pharmacokinetic profiles. Water-soluble polymers offer the potential to improve the pharmacokinetic profiles of these cytotoxic drugs by decreasing the volume of distribution, prolonging the elimination phases, making hydrophobic molecules water-soluble and releasing drug molecule slowly to result

high intratumoral drug level. Cytotoxic drugs that are covalently attached to water-soluble polymers via reversible linkages more effectively target tumor tissue than the drugs alone [25].

In drug–polymer conjugates, drug is linked to polymers covalently. It is obvious that the molecular mass and physico-chemical properties of the polymer are the most important considerations acting on biodistribution, elimination and metabolism of the conjugate. Thus, the choice of an appropriate polymer is vital. In each case, non-toxic, non-immunogenic water-soluble polymer which is suitable for repeated administration must be chosen [polymer conjugates]. Finally, the carrier should possess convenient functional groups for attaching the respective drug or spacer.

Polymer–drug conjugates are composed of three main components; polymer backbone, polymer–drug linker and drug molecule [Figure 1.14] [26]. Also imaging agents and targeting residues are often added giving a very complex architecture. In addition, solubilizing groups can be attached to the polymeric carrier to modify the bioavailability of the conjugate.

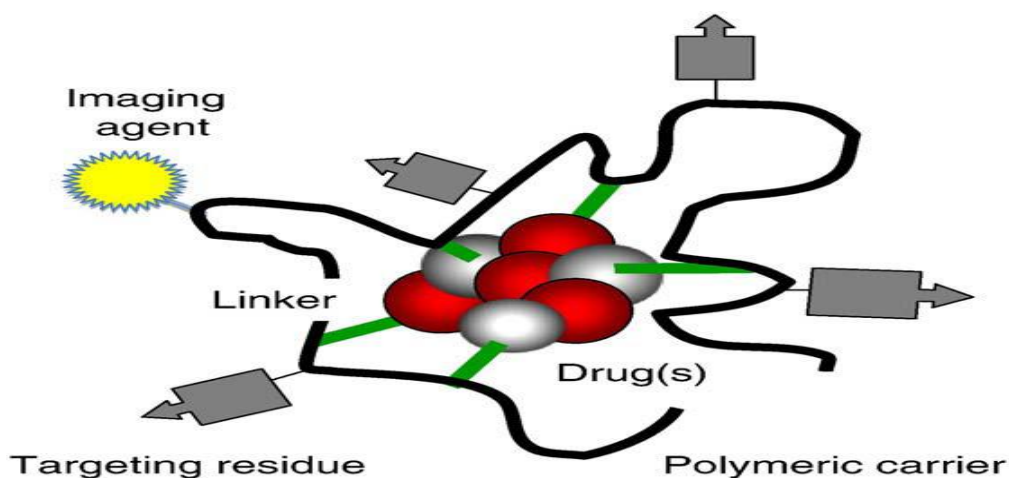


Figure 1.14 Schematic representation of polymer-drug conjugate [26]

Polymer-drug conjugates passively target solid tumor tissue because of a combination of reduced renal clearance and exploitation of the enhanced permeation and retention (EPR) effect. The Enhanced Permeability and Retention (EPR) effect is the property by which certain sizes of molecules, like macromolecular drugs, tend to accumulate in tumor tissue much more than they do in normal tissues [Figure 1.15] [27]. The reason for this phenomenon is that, tumor cells are usually abnormal in form and architecture with no smooth muscle layer.

Furthermore, tumor tissues usually lack effective lymphatic drainage. All these factors stimulate macromolecular drugs to be transport through tumor cells. The EPR effect is important for nanoparticle and liposome delivery to cancer tissue.

In one of the studies, by Singer J. W. a polymer-drug conjugate, PPX is designed to enhance the efficacy and safety of anti-cancer agent, paclitaxel by improving its pharmacokinetical profile and to provide a water-soluble alternative to the standard paclitaxel formulation through conjugation to a biodegradable, water soluble polymer, poly-l-glutamic acid [Figure 1.16] [28]. The pharmacokinetic profile of PPX and standard paclitaxel are compared. It is observed that the total taxane Cmax and AUC values were significantly higher in PPX administered trials which indicates that paclitaxel with poly-l-glutamic acid polymer backbone has a prolonged circulation in the plasma and negligible release of the active agent, paclitaxel [Table 1.2] [28]. This prolonged circulation allowed for higher concentrations of the drug-conjugate to accumulate in the tumor vasculature.

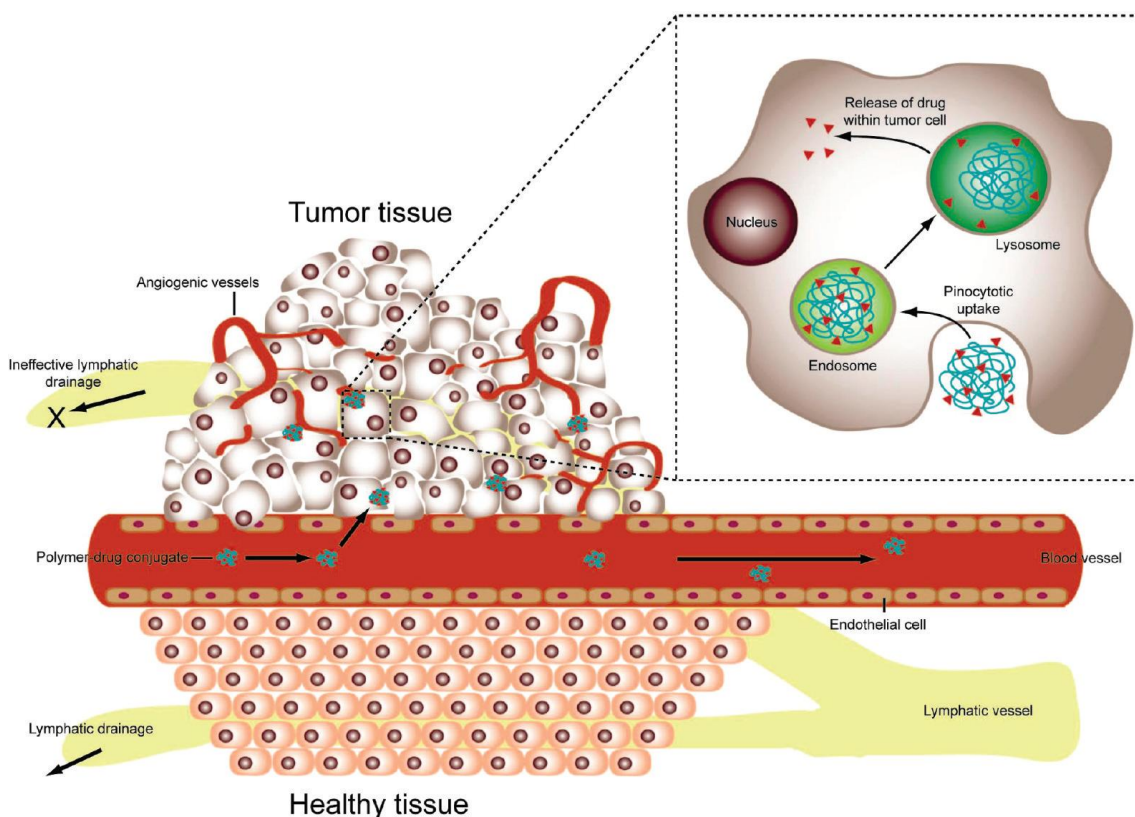


Figure 1.15 Schematic representation of EPR effect [27]

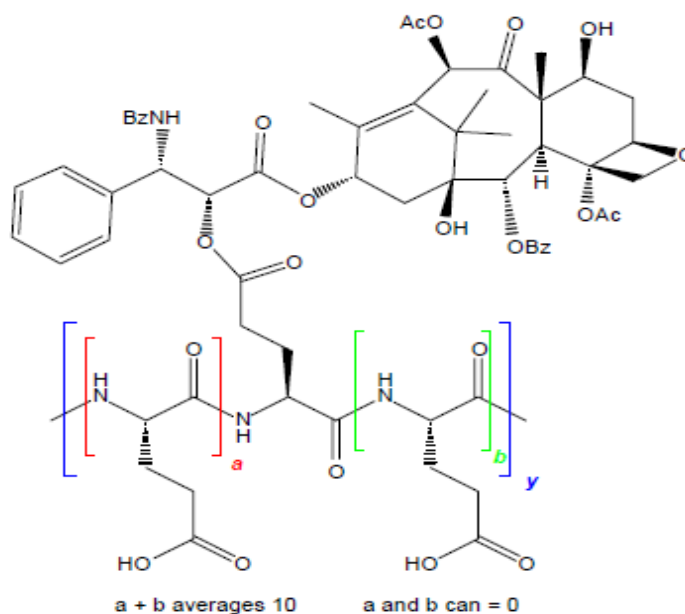


Figure 1.16 Structure of PPX [28]

Table 1.2. Pharmacokinetic Properties of PPX and Standard Paclitaxel [28]

	Plasma	
	C_{\max} ($\mu\text{g/mL}$)	$\text{AUC}_{0-\text{last}}$ ($\mu\text{g/mL} \cdot \text{h}$)
<i>PPX</i>		
Total taxanes	1081	4533
Extractable taxanes	2.1	18.1
Free paclitaxel	1.6	5.4
<i>Standard paclitaxel</i>		
Total taxanes	418	374
Extractable taxanes	424	297
Free paclitaxel	421	271

Plasma concentrations of PPX and free paclitaxel are also compared [Figure 1.17] [28]. In human PK studies, the plasma concentrations of PPX decrease biophysically. It has a prolonged distribution phase, and the apparent terminal phase that is associated with drug elimination is about 48 hours. Traces of drug molecule can still be observed in the plasma 3 weeks after its administration and plasma concentration decreases in a bi-exponential fashion in parallel to the parent drug concentrations [28].

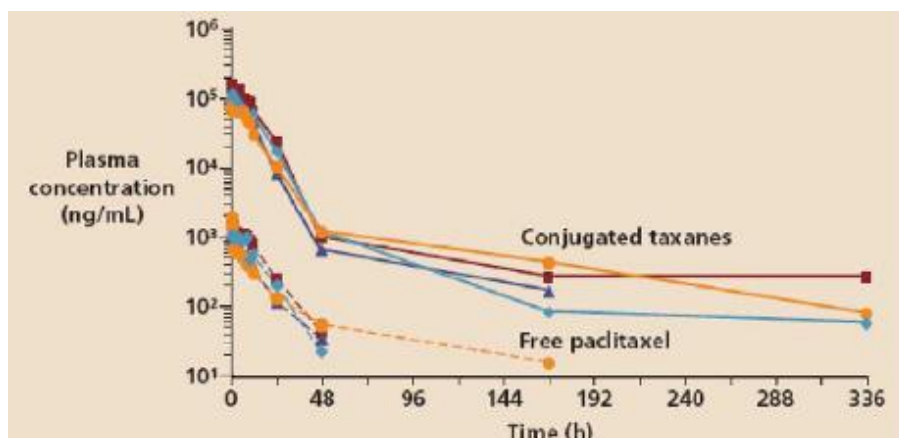


Figure 1.17 Plasma concentration of taxane [28]

Eventually, tumor exposure to total paclitaxel is greater in PPX trials than in those treated with paclitaxel. The distribution of paclitaxel to tumor tissue is faster with paclitaxel [Figure 1.18] [28]. However, overall tumor exposure to extractable paclitaxel is greater with PPX. The tumor concentration of total paclitaxel is 32% greater at 144 h after the administration of PPX [28].

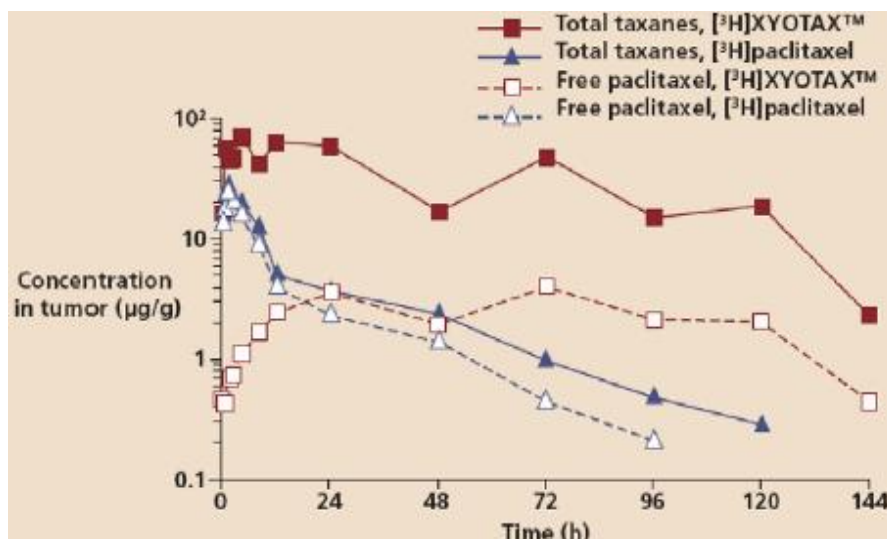


Figure 1.18 Tumor concentration of taxane [28]

Through the clinical development of polymer–anticancer drug conjugates, polymer therapeutics is becoming well established as a new class of therapy for cancer treatment.

2. AIM OF THE STUDY

The aim of the study is to synthesize an anti-angiogenesis agent and attach a linker to this drug molecule for future conjugation of the drug to macromolecules [Figure 2.1]. The cellular activity of the synthesized drug and intermediate molecules will be examined *in vitro*.

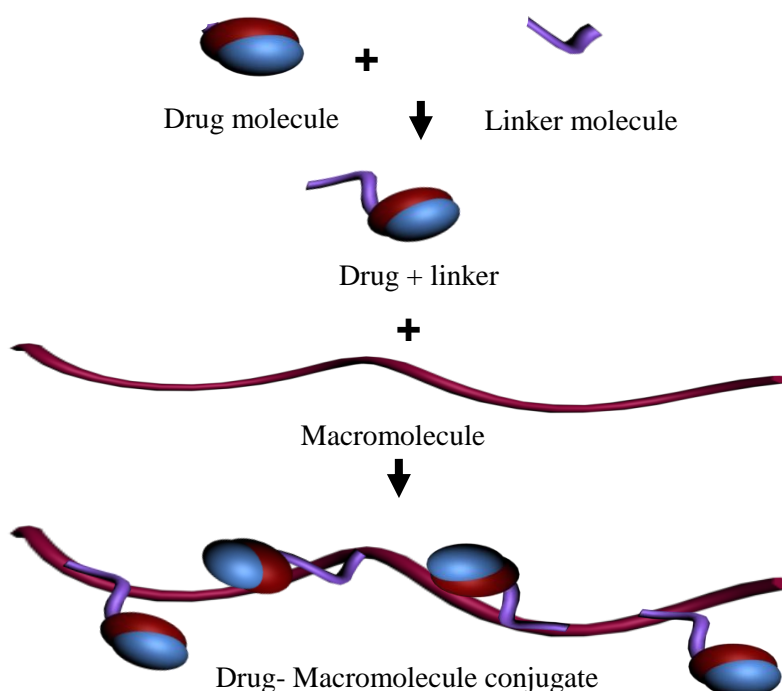


Figure 2.1 Schematic representation of functionalized drug-macromolecule conjugate

Conjugation of drugs to macromolecules brings in the advantage of increasing accumulation in the tumor, therefore increasing the amount of drug in the tumor. In the meantime, due to the decreased activity of the drug because of polymer conjugation, the effect of the polymer-bound drug to normal cells is diminished, decreasing the potential side effects. After reaching the site of interest, the drug will get released from the macromolecule exhibiting the anti-angiogenic effect. Combretastatin A-4, preventing the growth of tumor cells by destroying the existing vasculature of tumors by binding to tubulin, is chosen as the angiogenesis inhibitor for this study.

3. RESULTS AND DISCUSSION

The project is composed of two parts:

- a. Synthesis of Combretastatin A-4 (**1**)
- b. Synthesis of Amino Analog (**4**) of CA-4

Followed by the synthesis of CA-4 (**1**), various methods for the synthesis of the amino functionalized CA-4 (**4**) was examined [Figure 3.1]. There are three major routes explored for the synthesis of the amino derivative. The steps of the synthesis and the methods used to reach the final goal of synthesis of molecule **4** are explained in the following sections.

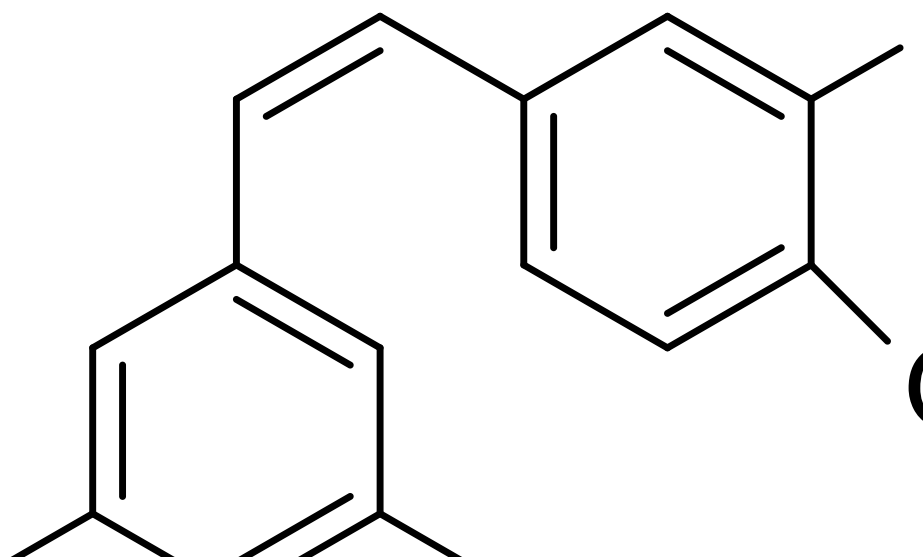


Figure 3.1 Schematic representation of the synthesis of CA-4 analogues

3.1. Synthesis of Cis-Combretastatin A-4

Propenoic acid **13** was obtained via the reaction of 3-hydroxy-4-methoxybenzaldehyde **11** and 3,4,5-trimethoxyphenylacetic acid **12** in presence of acetic anhydride and

triethylamine [Figure 3.2]. Purity of the product was examined with HPLC (95 %) and characterized via ^1H NMR spectrum [Figure 3.3 and 3.4 respectively].

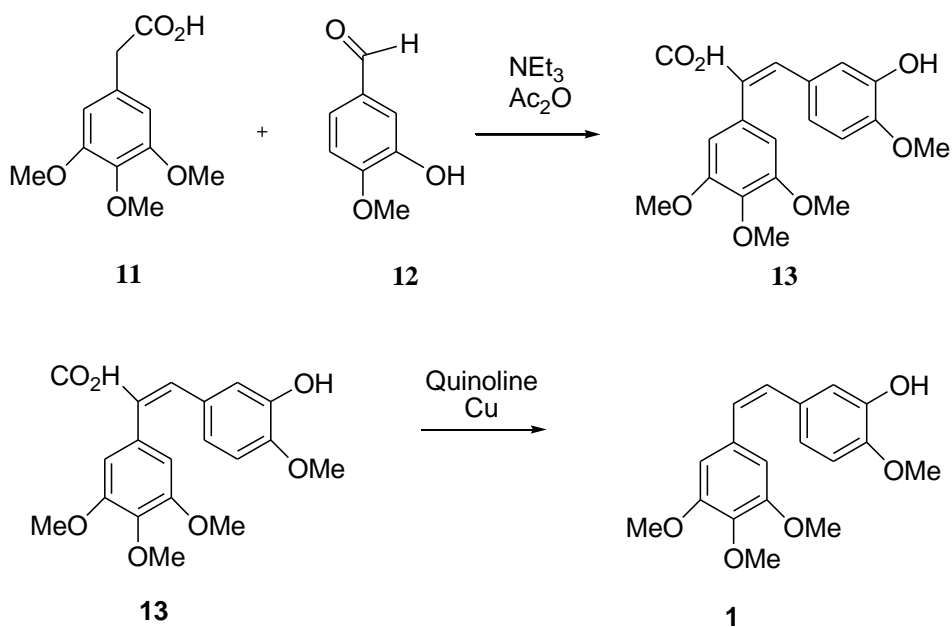


Figure 3.2 Synthesis of propenoic acid intermediate **13** and Combreastatin A-4 **1**

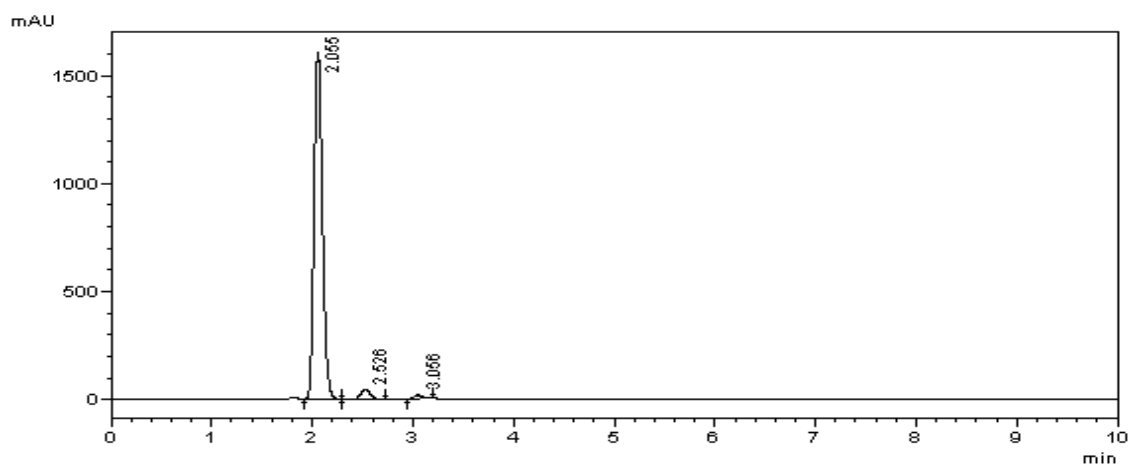


Figure 3.3 HPLC spectrum of propenoic acid **13**

There are three different methoxy groups and twelve H's attached to these methoxy groups appear at 3.68, 3.72 and 3.74 ppm. Aromatic protons appear at 6.44, 6.54, 6.80 and 7.58 ppm and the vinylic proton appears at 6.61 ppm. Carboxylic acid proton appears at 12.38 ppm in DMSO-d_6 .

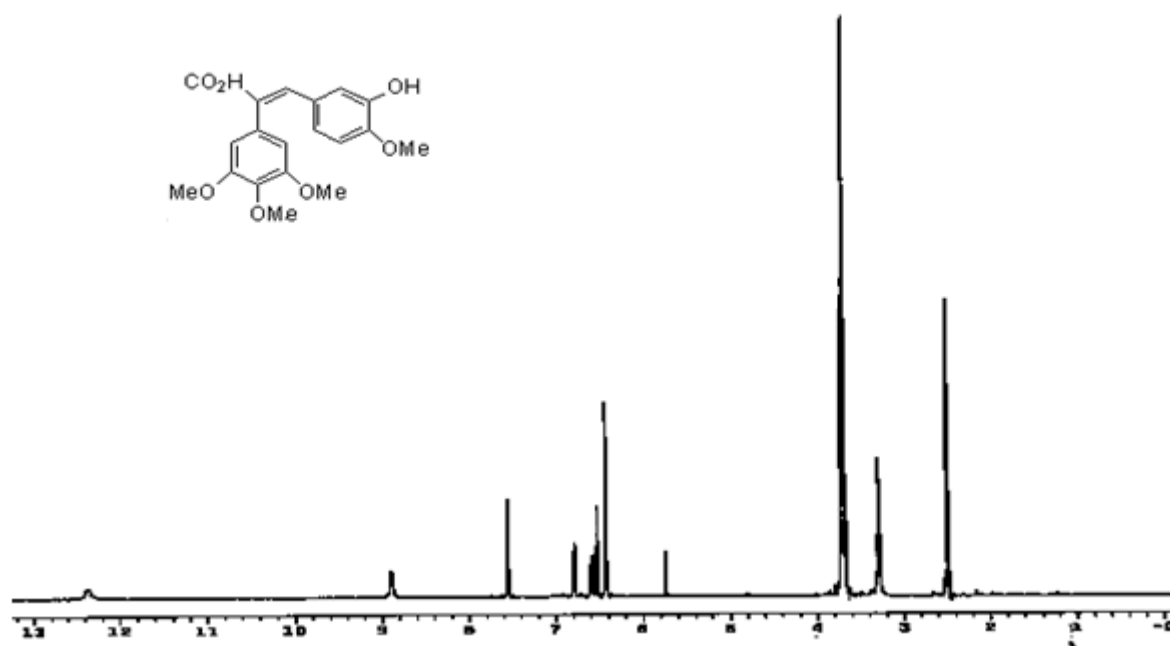


Figure 3.4 ^1H NMR of propenoic acid **13**

Combretastatin A-4 **1** was synthesized via the decarboxylation of the propenoic acid (**13**) in the presence of copper and quinoline with 60 percent yield [Figure 3.2]. The product was characterized via ^1H NMR spectrum and the purity was examined with HPLC (95 %) To detect and see the purity of the product, HPLC and ^1H -NMR spectra were used [Figure 3.5 and 3.6 respectively].

The peak at 12.38 that appears due to the carboxylic proton in ^1H NMR of **13** [Figure 3.4], disappears and the second vinylic proton after the decarboxylation reaction appears at 6.45 ppm.

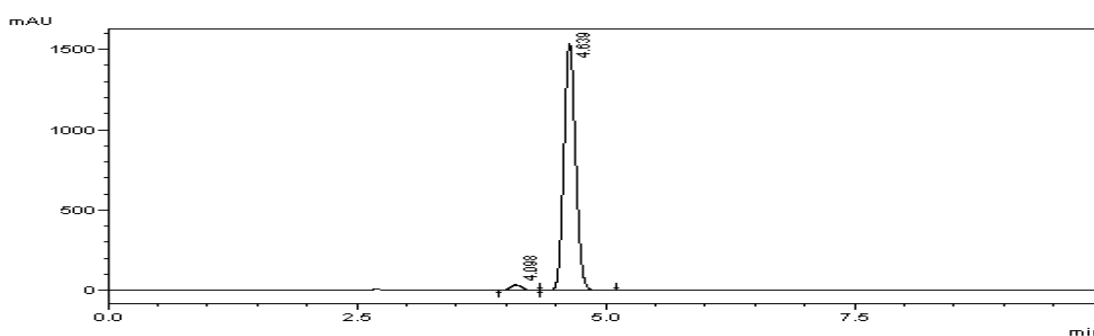


Figure 3.5 HPLC spectrum of CA-4 **1**

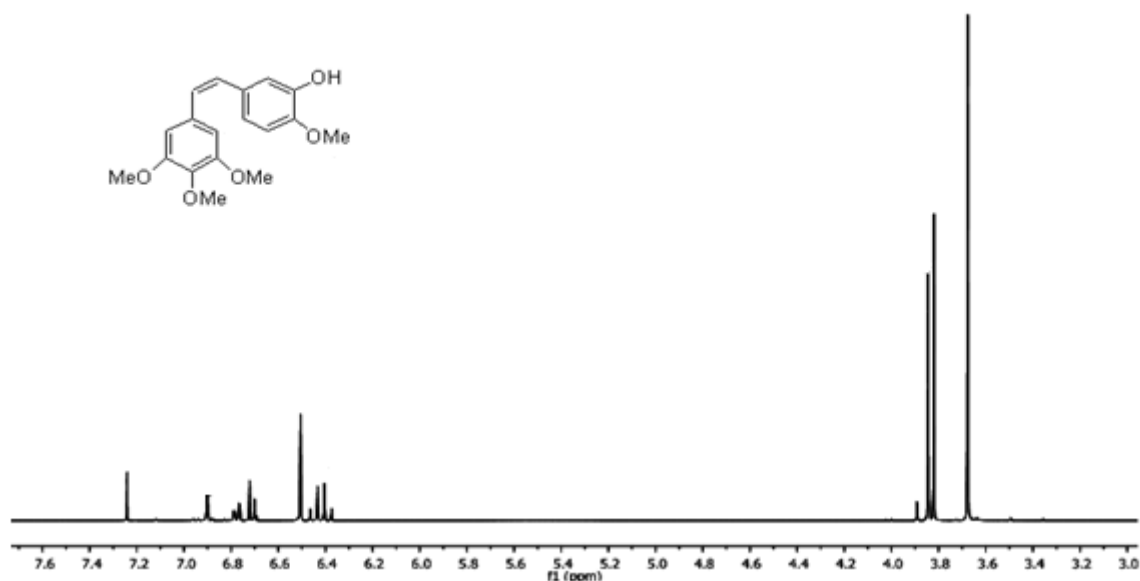


Figure 3.6 ^1H NMR spectrum of CA-4 **1**

3.2 Functionalization of Cis-Combretastatin A-4

For covalent attachment of drug molecules to the macromolecule the drug molecule should bear amine functionality. The complimentary functional group on the polymer for the amine bearing drug molecule would be N-hydroxy succinic anhydride group, resulting an amide bond after the conjugation [Figure 3.7].

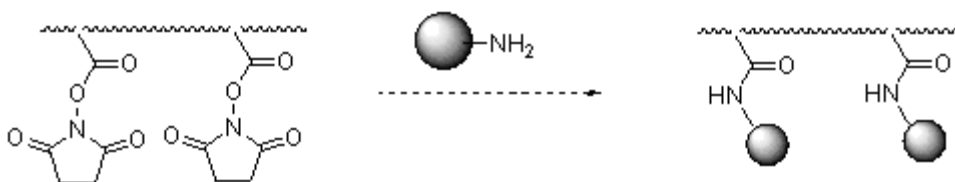


Figure 3.7 Schematic representation of drug- macromolecule conjugation

A total of three different routes were examined to obtain the desired amino molecule **4** [Figure 3.1]. The first route is the attachment of the protected glycine, followed by the deprotection reaction to obtain analog **4** [Figure 3.8]. The reaction of CA-4 molecule **1** with

BOC-Gly-OH **2** by DCC/DMAP coupling in CH_2Cl_2 is to synthesize a protected amine-functionalized molecule **3** [Figure 3.8].

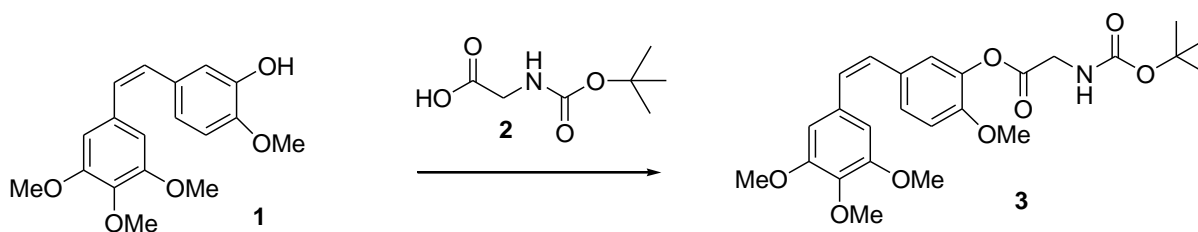


Figure 3.8 Reaction of CA-4 with BOC-Gly-OH **3**

HPLC spectrum showed that the retention time for the product is 10.56 min. and the purity was 98.1 percent.

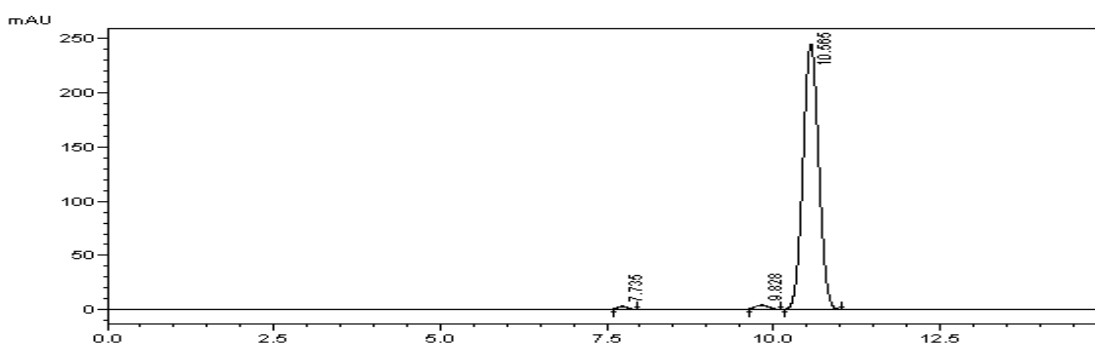


Figure 3.9 HPLC spectrum of the molecule **3**

The purity was determined by HPLC and the product was characterized by $^1\text{H-NMR}$ spectrum [Figure 3.9 and 3.10]. Nine protons due to the t-BOC protecting group appear at 1.45 ppm. Methylene protons present due to the newly attached group appear at 3.91 ppm. Yield of the reaction was 74 percent.

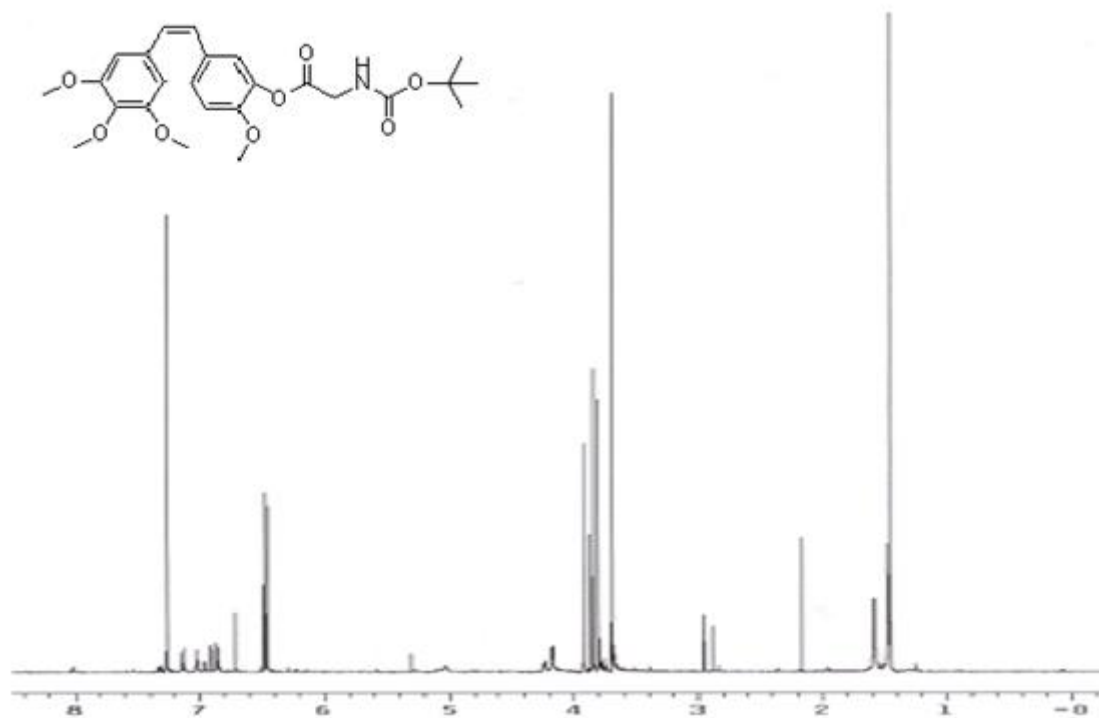


Figure 3.10 ^1H NMR spectrum of the molecule **3**

For the deprotection reaction, primarily trifluoroacetic acid was used under dry conditions. Since the product was not obtained as pure as necessary, the deprotection reaction was tried with oxalyl chloride in dry methanol [Figure 3.11]. The reaction was monitored by FTIR and HPLC [Figure 3.12, 3.13].

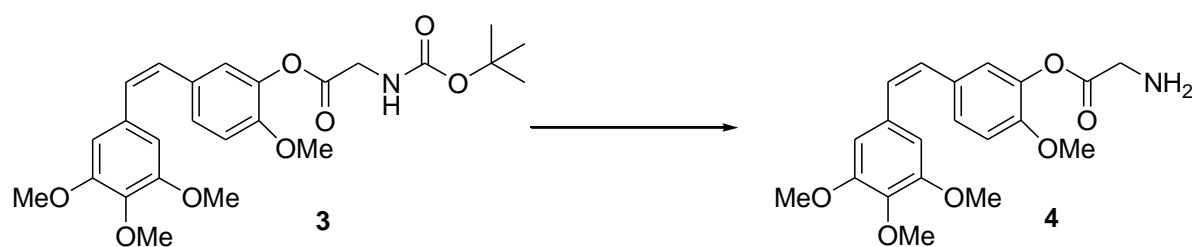


Figure 3.11 Deprotection reaction of amine **4**

In the FTIR spectrum, the newly forming broad peak at 3403 cm^{-1} is due to the amine group, and the peak at 1775 cm^{-1} is due to the carboxyl group of the product.

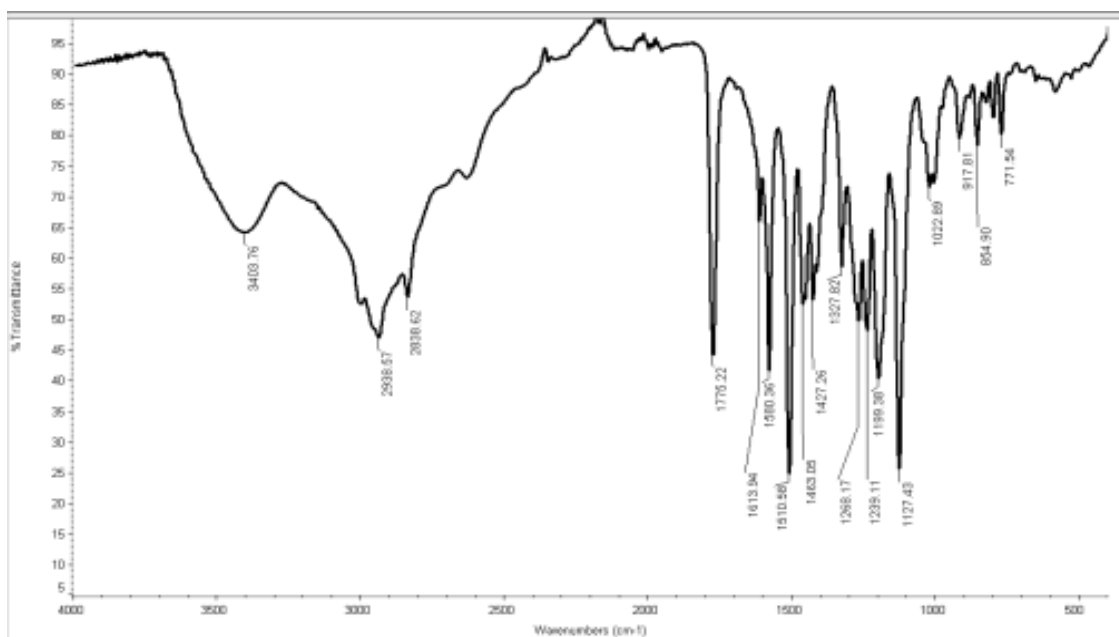


Figure 3.12 FTIR spectrum of amine-terminated CA-4 molecule **4**

After purification HPLC spectrum showed that the product was 97.5 percent pure and the retention time is 1.276 min. The yield of the product was very low (10 percent), so different methods were tried to functionalize CA-4 molecule.

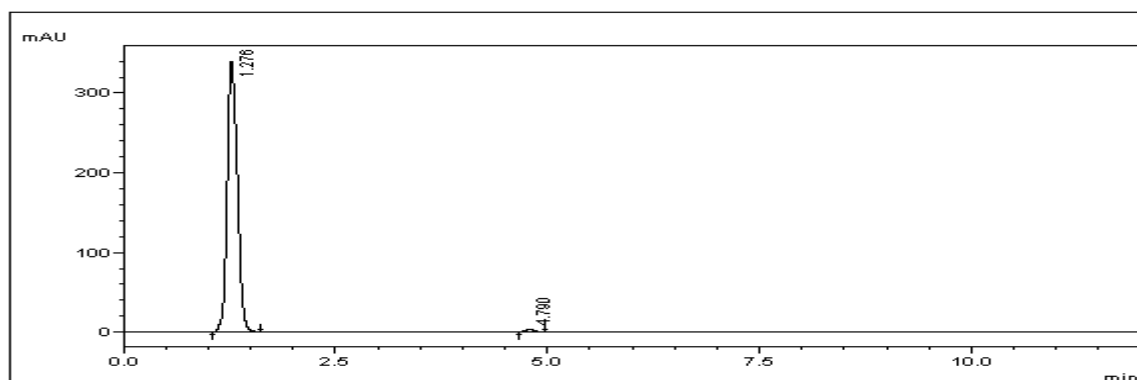


Figure 3.13 HPLC of molecule **4**

The second route utilized involved Gabriel amine synthesis. Gabriel synthesis is a chemical reaction that transforms primary alkyl halides into primary amines using a two step procedure potassium phthalimide and hydrazine. The attachment of the phthalimide group was accomplished through a two step procedure where a bromo containing molecule **5** was

attached to CA-4 and subsequently converted to the phthalimide. For Gabriel synthesis, first CA-4 **1** was reacted with bromoacetic acid (**5**) via DCC coupling at room temperature to obtain a halide terminated CA-4 molecule **6** [Figure 3.14].

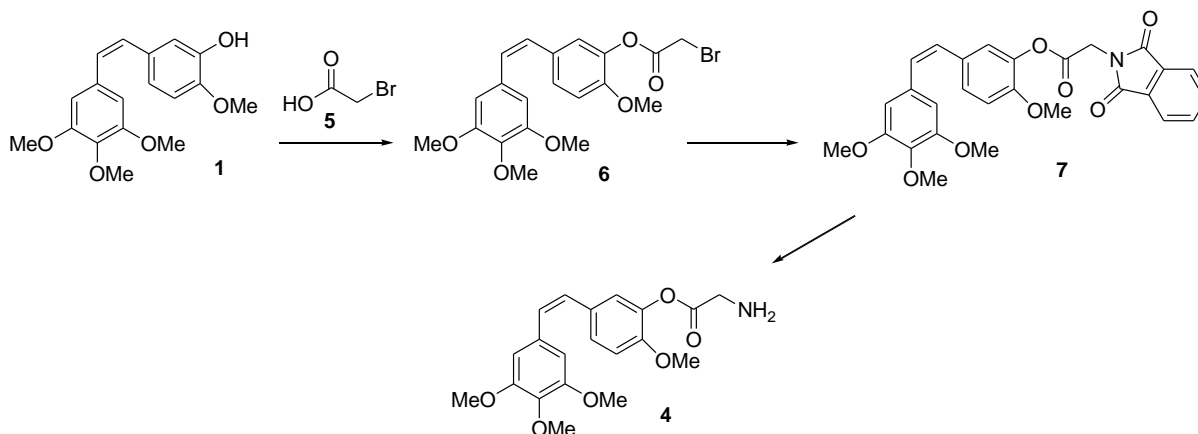


Figure 3.14 Gabriel synthesis

Following the purification, ^1H NMR spectrum analysis showed the newly forming methylene protons at 4.02 ppm [Figure 3.15]. HPLC spectrum showed that the retention time of the product was 9.78 min. and the purity was 90.1 percent [Figure 3.16].

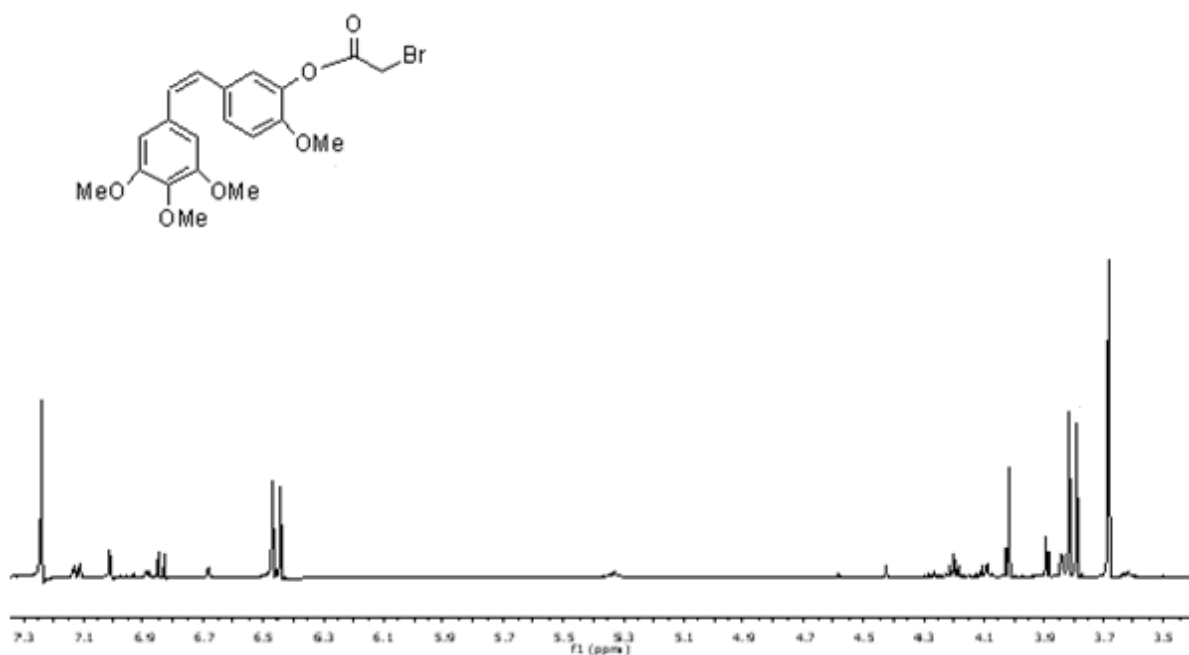


Figure 3.15 ^1H NMR of molecule **6**

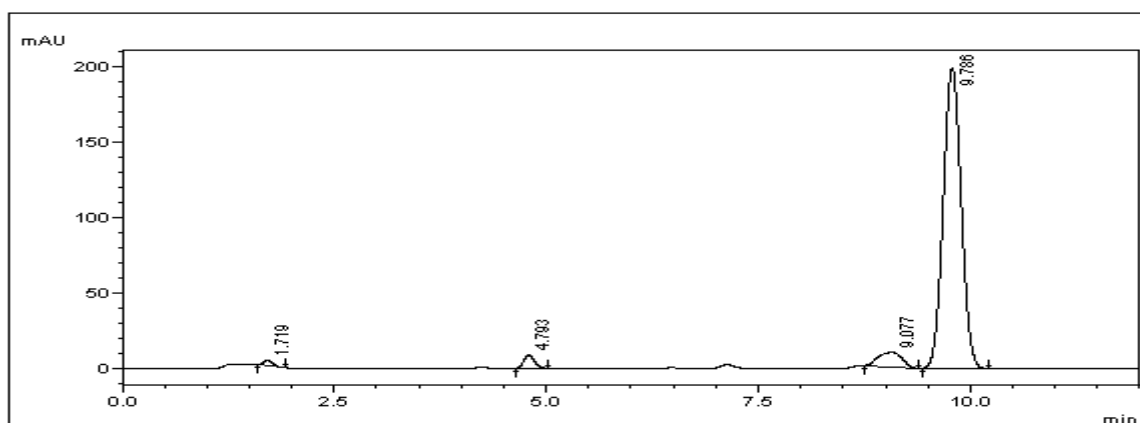


Figure 3.16 HPLC of molecule **6**

After the formation of bromine-ended CA-4 molecule **6**, it was reacted with potassium phthalimide in acetonitrile at 90 °C [Figure 3.16]. After the reaction was completed, the product **7** was analyzed via $^1\text{H-NMR}$ and HPLC.

Appearance of the new peaks at 7.88 and 7.74 ppm due to the aromatic protons of the phthalimide and at 4.66 ppm due to the methylene protons confirmed the formation of the desired product [Figure 3.17].

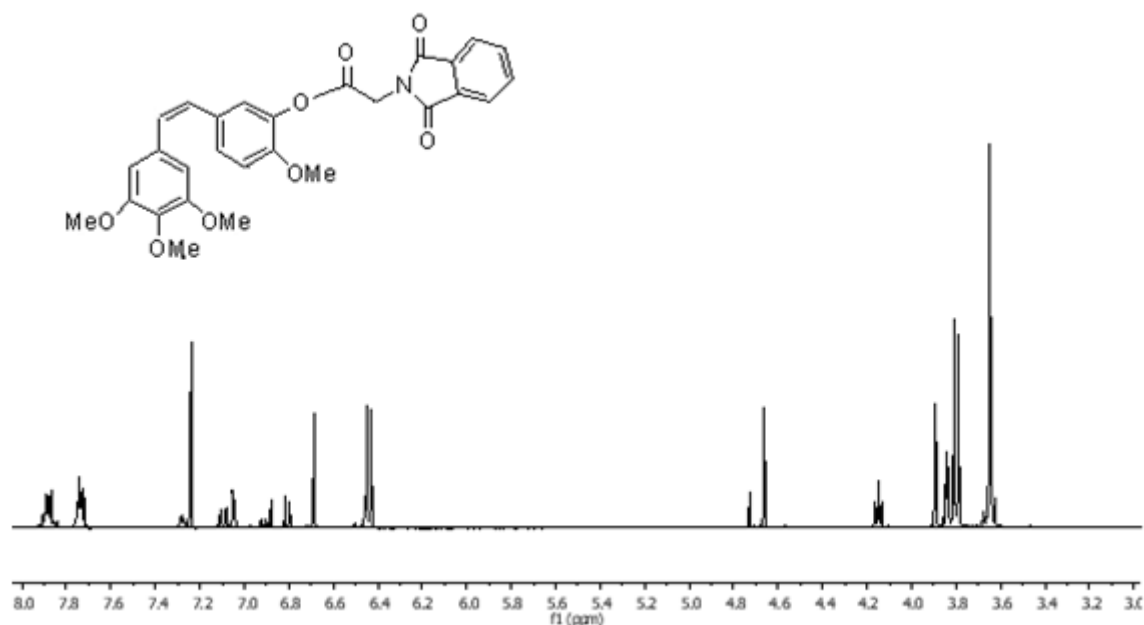


Figure 3.17 $^1\text{H-NMR}$ of the molecule **7**

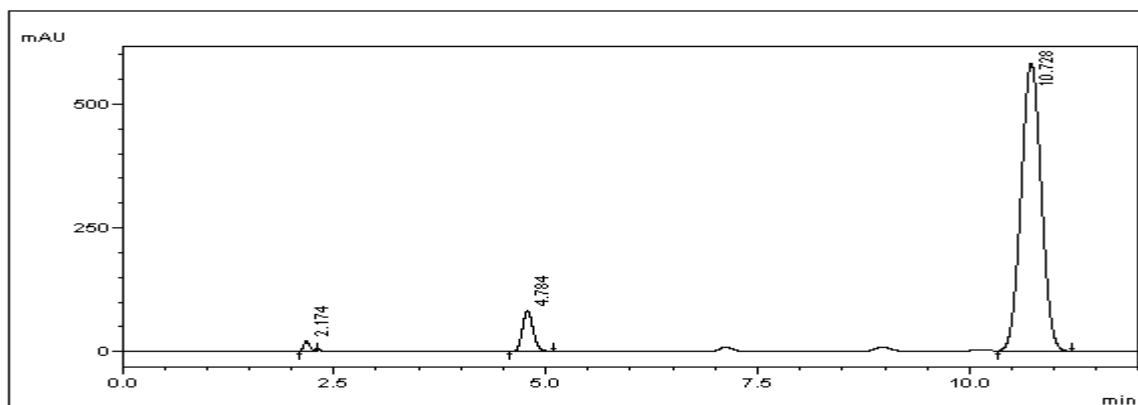


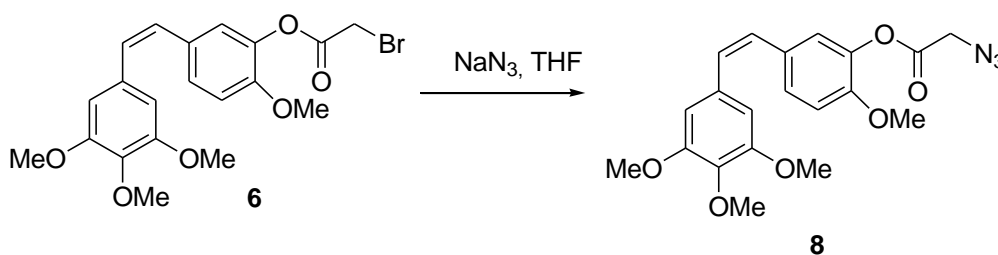
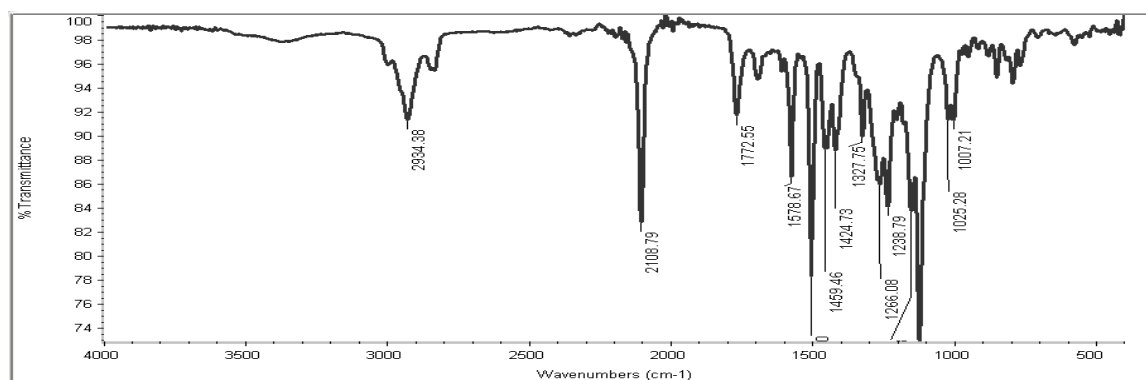
Figure 3.18 HPLC of the molecule **7**

Additionally, HPLC analysis was done to examine the purity [Figure 3.18]. The retention time of the product is 10.72 min. And the purity is 92 percent.

The last step of the Gabriel amine synthesis was accomplished via the treatment of phthalimide analog **7** with hydrazine hydrate in ethanol [Figure 3.14]. ^1H NMR spectrum analysis of the product showed evidence of hydrolysis of the ester bond. No desired product was obtained from this reaction, but starting CA-4 molecule was recovered.

The third route examined for the synthesis of amine terminated CA-4 analog was the Staudinger reduction. In the Staudinger reaction the combination of an azide with a phosphine or phosphite produces an iminophosphorane intermediate. The hydrolysis of the aza-ylide produces a phosphine oxide and an amine. Commonly, triphenylphosphine is used as the reducing agent, yielding triphenylphosphine oxide as the side product in addition to the amine.

In this experiment, bromo-terminated CA-4 molecule **6** was reacted with sodium azide at 55 °C [Figure 3.19]. After purification, the product was characterized by FTIR spectrum [Figure 3.20]. The peak at 2108 cm^{-1} is due to the azide group and the carbonyl stretch appears at 1772 cm^{-1} .

Figure 3.19 Synthesis of azide-terminated CA-4 molecule **8**Figure 3.20 FTIR spectrum of azide-terminated CA-4 molecule **8**

Second step of the proposed route was the reduction of azide to amine. For this reaction, triphenylphosphine was used to reduce the azide-terminated product **8** in THF/water mixture [Figure 3.21]. The reaction was followed by TLC and ¹H-NMR, but the desired product could not be observed.

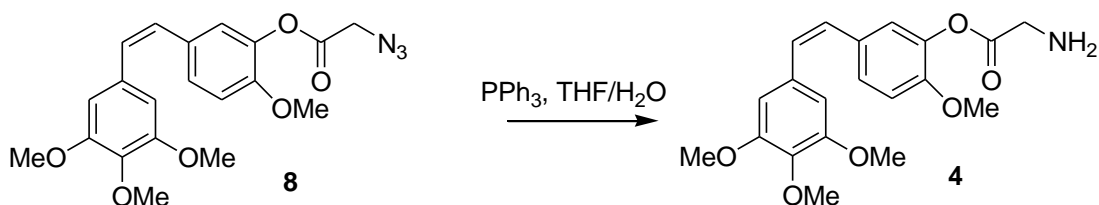


Figure 3.21 Staudinger reduction

Eventually, Staudinger reduction was tried to another azide-terminated CA-4 molecule with a longer alkyl chain between azide and carboxyl group obtained by DCC coupling of CA-4 molecule with 4-azidobutanoic acid (**9**) [Figure 3.22].

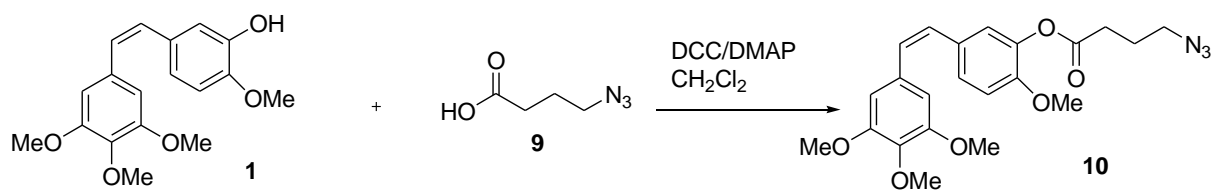


Figure 3.22 Synthesis of the molecule **10**

The reaction was followed via ¹H-NMR and HPLC spectra. ¹H-NMR spectrum confirms the occurrence of the reaction. The methylene protons appeared at 3.41, 2.63 and 1.97 ppm [Figure 3.23]. HPLC spectrum exhibits that the retention time of the molecule is 12.734 min. The purity after purification is 95.5 percent [Figure 3.24].

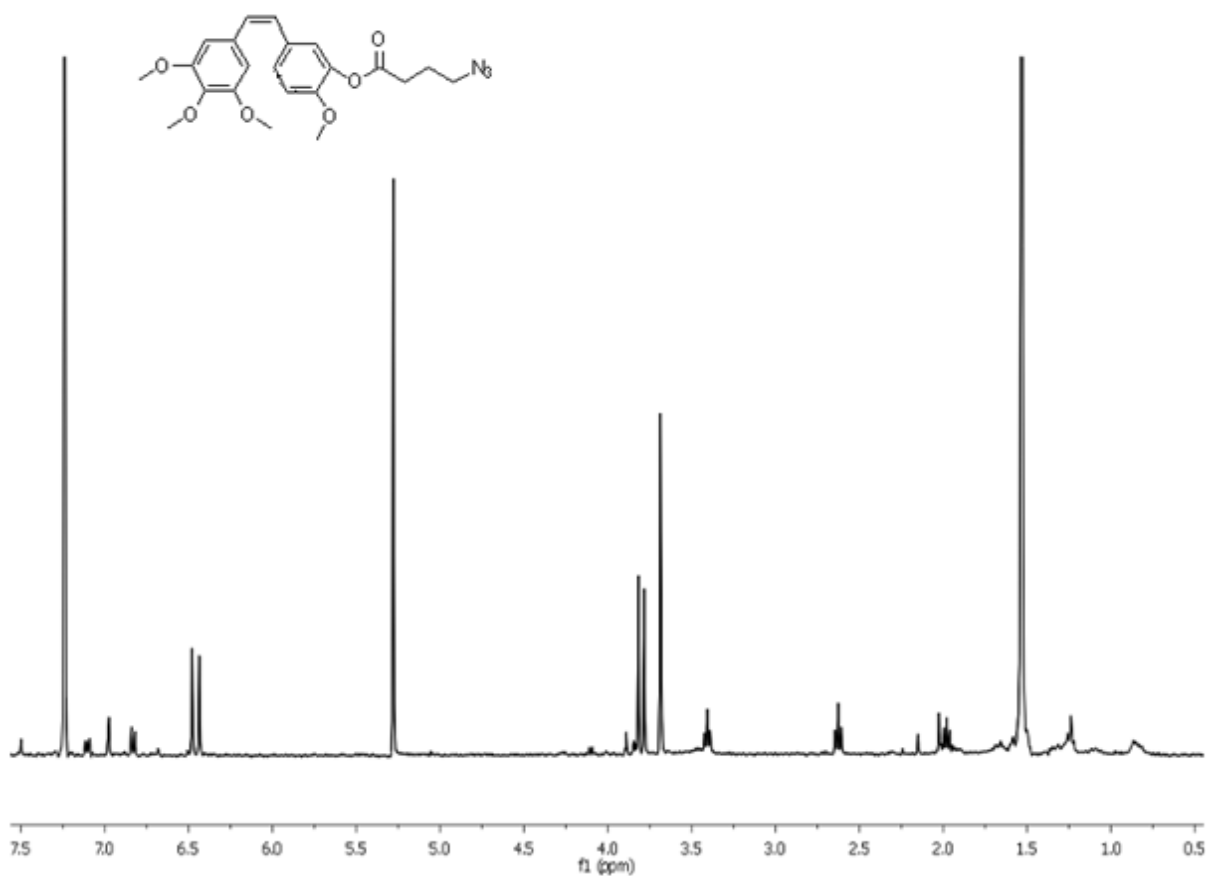


Figure 3.23 ¹H NMR of the product **10**

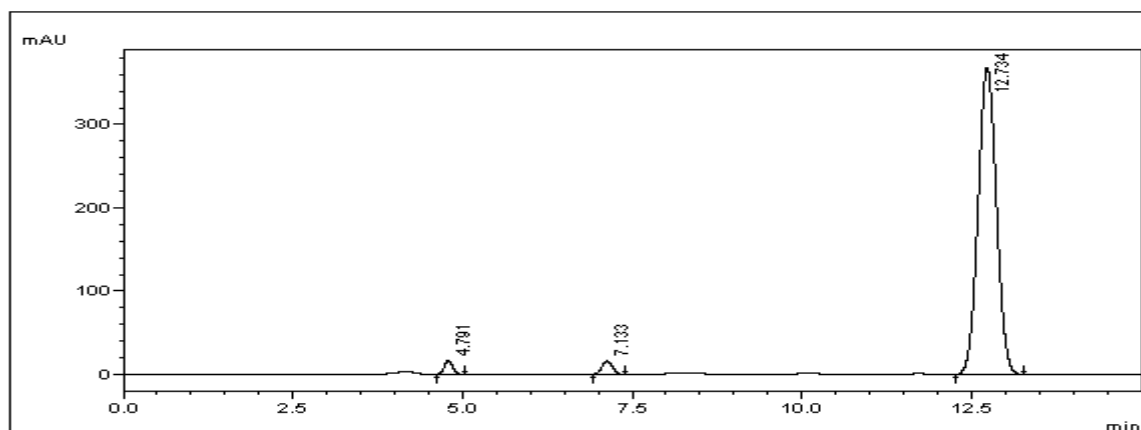


Figure 3.24 HPLC of the product **10**

For the last step, again Staudinger reduction was tried by the addition of triphenylphosphine to azide-functionalized CA-4 molecule **4** [Figure 4.27]. However, again the labile ester bond hydrolysis was the main course of the reaction. The desired product could not be obtained.

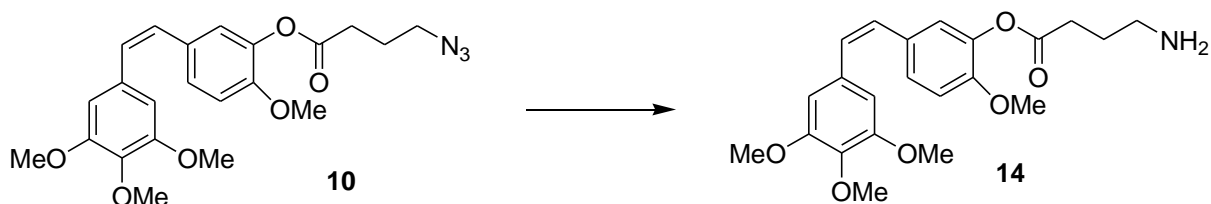
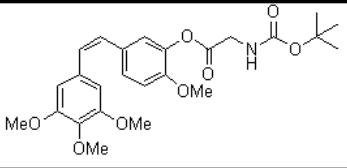
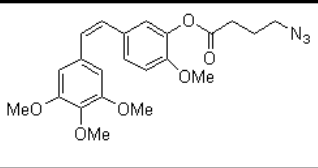
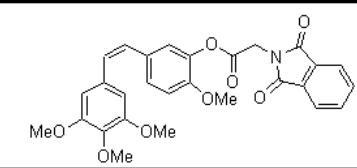
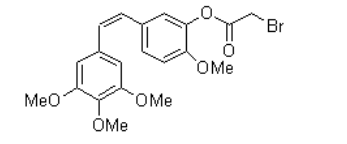
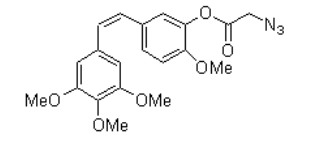
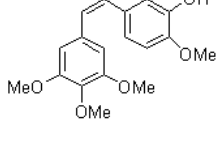
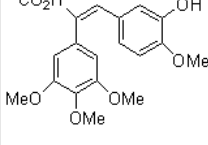


Figure 3.25 Reduction of the molecule **10**

With the impressive activity of CA-4 molecule against human umbilical vascular endothelial cells (HUVECs), these new analogs were tested for their HUVEC activity. Obtained IC₅₀ values are listed in the table

Table 3.1. IC50 values of CA-4 analogs (nM)

			
2.47	8.21	4.54	
			
14.57	24.99	4.45	3.68

In conclusion, different methods were applied to functionalize CA-4 anti-angiogenesis agent. Although the aim was to synthesize an amine-terminated agent, a route with a good yield of the desired molecule was not possible. Yet, during the course of this endeavor different analogues of CA-4 molecule were produced.

4. EXPERIMENTAL

4.1. Methods and Materials

All chemicals were used as received from manufacturer (Merck, Aldrich, Alfa Aesar, Riedel de Haen). Dry solvents (CH₂Cl₂, THF) were obtained from ScimatCo Purification System, other solvents were dried over molecular sieves. Column chromatography was performed using silicagel-60 (43-60 nm). Thin layer chromatography was performed using silica gel plates (Kiesel gel 60 F254, 0.2mm, Merck). Plates were viewed under 254 nm UV lamp. High Pressure Liquid Chromatography (HPLC) was performed with Shimadzu LC-20 AT with ACN:Water (65:35) solvent system and preparative HPLC was performed with LC-6 AD. Infrared spectroscopy was carried out on Thermo Scientific Nicolet 380 FT-IR spectrophotometer. ¹H NMR (operating at 400 MHz) was recorded on Varian Mercury-MX in CDCl₃ and DMSO-d₆ as solvent at the Advanced Technologies Research and Development Center at Boğaziçi University.

4.2. Synthesis

4.2.1. Synthesis of Cis Combretastatin A-4

Synthesis of Cis Combretastatin A-4 was a two-step reaction and it was synthesized according to the literature procedure [53].

4.2.1.1. Synthesis of E-2-(3',4',5'-Trimethoxyphenyl)-3-(3'-hydroxy-4'-methoxyphenyl) prop-2-enoic acid 13. E-2-(3',4',5'-Trimethoxyphenyl)-3-(3'-hydroxy-4'-methoxyphenyl) prop-2-enoic acid was synthesized according to the literature procedure. A mixture of 3-hydroxy-4-methoxybenzaldehyde **12** (0.67 g, 4.4 mmol), 3, 4, 5-trimethoxyphenylacetic acid **11** (2 g, 8.84 mmol) acetic anhydride (4 mL) and triethylamine (2 mL) were heated under reflux for 3 h. After acidification with concentrated hydrochloric acid (6 mL), the resulting solid was filtered off and recrystallised from ethanol to give propenoic acid **13** (950 mg, 60%) as fine yellow needles. ¹H-NMR (400 MHz, δ, DMSO-d₆): 3.68 (6 H, s), 3.72 (3 H, s), 3.74

(3H, s), 6.44 (2 H, s), 6.54 (1 H, s), 6.61 (1 H, d, $J = 8$ Hz), 6.80 (1 H, d, $J = 8$ Hz), 7.58 (1 H, s).

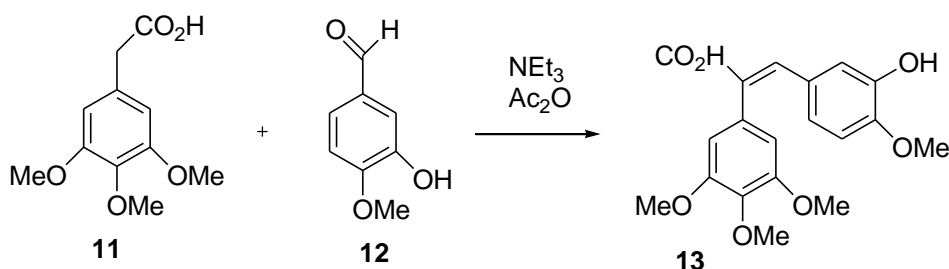


Figure 4.1. Perkin Condensation of 3,4,5-Trimethoxyphenylacetic Acid **11** and 3-Hydroxy-4-methoxybenzaldehyde **12**

4.2.1.2. Synthesis of Combretastatin A-4 **1** by Decarboxylation of Cinnamic Acid. Cis Combretastatin A-4 **1** was synthesized according to the literature procedure [53]. (*E*)-3-(3'-Hydroxy-4'-methoxyphenyl)-2-(3'',4'',5''-trimethoxyphenyl)prop-2-enoic acid **13**, (2 g, 5.56 mmol) was added to powdered copper (1.84 g, 28.8 mmol) in quinoline (20 mL, 21.9 g, 0.17 mol), and the resulting mixture was heated at 200 °C for 2 h. Upon cooling, ether was added, and the copper was filtered off through Celite. The filtrate was washed with 1 M hydrochloric acid, and the aqueous layer was separated and extracted with ether. The combined organic layers were washed with saturated aqueous sodium carbonate, water, brine, dried (Na_2SO_4), and concentrated in *vacuo*. Flash column chromatography and recrystallization from ethyl acetate and hexane afforded cis combretastatin A-4 (**1**) as a pale yellow crystalline solid (1.19 g, 68%). ^1H NMR (CDCl_3 , δ , ppm); 3.68 (6H, s), 3.82 (3H, s), 3.84 (3H, s), 6.39 (1H, d, $J = 6$ Hz), 6.45 (1H, d, $J = 6$ Hz), 6.51 (2H, s), 6.71 (1H, d, $J = 5.2$ Hz), 6.77 (1H, dd, $J = 3.2, 5.2$ Hz), 6.90 (1H, d, $J = 3.2$ Hz). FTIR (cm^{-1}); 3418.6.

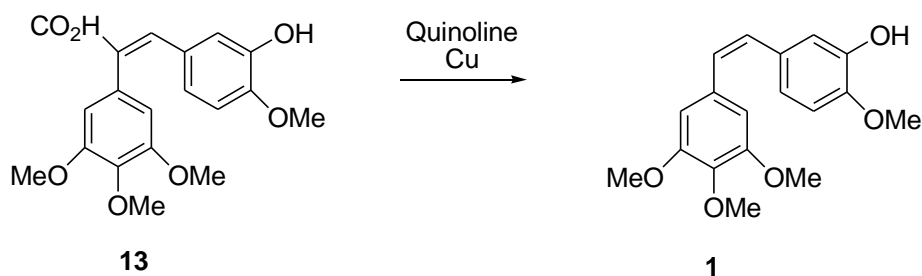


Figure 4.2. Synthesis of Combretastatin A-4 **1** by Decarboxylation of Cinnamic Acid

4.2.2. Synthesis of (Z)-5-(3,4,5-trimethoxystyryl)-2-methoxyphenyl 2-aminoacetate via deprotection of t-BOC derivative reaction

4.2.2.1. Synthesis of (Z)-5-(3,4,5-trimethoxystyryl)-2-methoxyphenyl2-(tert-butoxycarbonyl) acetate 3. To a solution of Combretastatin A-4 **1** (0.1 g, 0.32 mmol) dissolved in dry CH₂Cl₂ (5 mL), 2-(tert-butoxycarbonyl) acetic acid **2** (0.0664 g, 0.38 mmol) was added followed by DCC (0.0783 g, 0.38 mmol) and DMAP (0.0193 g, 0.16 mmol). After stirring at room temperature overnight for 12 h under nitrogen, the DCU was filtered off and washed with small amounts of CH₂Cl₂. Reaction mixture was extracted with 1 M NaHSO₄ (3 x 60 mL), 10 % Na₂CO₃ (3 x 60 mL) and then with brine (1x 60 mL). Combined organic layers were dried over anhydrous Na₂SO₄. The residue was concentrated in *vacuo*. ¹H NMR (CDCl₃, δ, ppm); 1.45 (9H, s) 3.69 (6H, s), 3.79 (3H, s), 3.83 (3H, s), 3.91 (2H, s), 6.45 (2H, s), 6.48 (2H, s), 6.86 (1H, d, *J* = 5.2 Hz), 7.01 (1H, d, *J* = 8 Hz), 7.14 (1H, dd, *J* = 5.2, 8 Hz). FTIR (cm⁻¹); 1778.62, 1714.72.

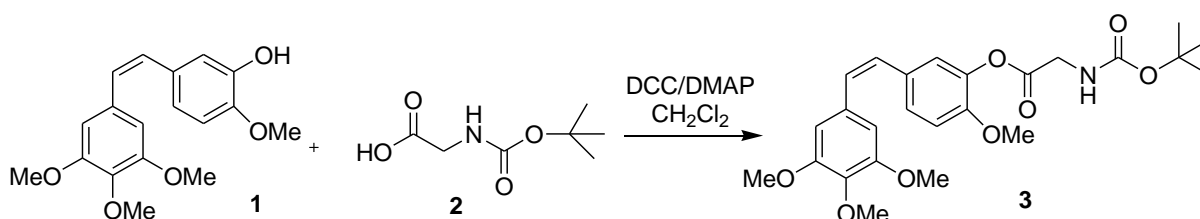


Figure 4.3 Synthesis of the molecule **3**

4.2.2.2. Synthesis of (Z)-5-(3,4,5-trimethoxystyryl)-2-methoxyphenyl 2-aminoacetate 4. (COCl)₂ (0.1 mL) was added to dry MeOH (1 mL) in an ice bath under nitrogen. (Z)-5-(3,4,5-trimethoxystyryl)-2-methoxyphenyl2-(tert-butoxycarbonyl) acetate **3** (0.05 g, 0.106 mmol) was dissolved in dry CH₂Cl₂ (5 mL). (COCl)₂ solution was injected transferred to (Z)-5-(3,4,5-trimethoxystyryl)-2-methoxyphenyl2-(tert-butoxycarbonyl) acetate solution at 0 °C and stirred for 2 h. at 0 °C. MeOH was evaporated at 10 °C in *vacuo*. CH₂Cl₂ was added (10 mL) and washed with NaHCO₃ (3 times x 10 mL). Organic layer was extracted with distilled water (3 x 10 mL) and dried over anhydrous Na₂SO₄. The residue was concentrated in *vacuo* and crude product was purified by prep-HPLC to give pure white solid product **4**, (0.004 g, 0.011 mmol, 97.5 percent purity, 10 percent yield). ¹H-NMR (400 MHz, δ, CDCl₃); 3.68 (6H, s),

3.78 (3H, s), 3.81 (3H, s), 3.91 (2H, s), 6.44 (2H, s), 6.45 (2H, s), 6.84 (1H, d, $J = 4$ Hz), 6.99 (1H, d, $J = 8$ Hz), 7.12 (1H, dd, $J = 4.0, 8.0$ Hz). FTIR (cm^{-1}) 3403.8, 1775.2

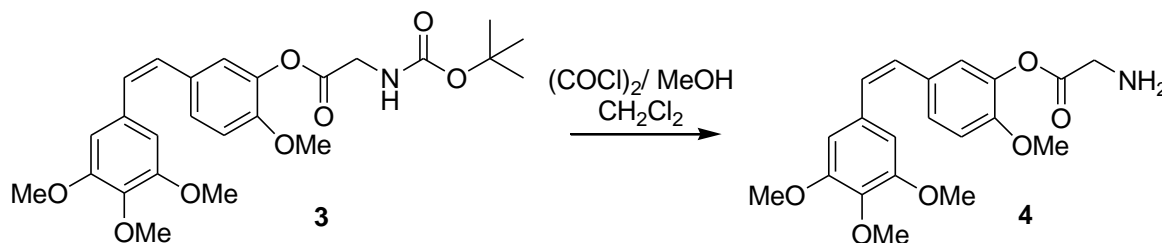


Figure 4.4 Synthesis of molecule 4 via deprotection of t-boc derivative

4.2.3. Synthesis of (Z)-5-(3,4,5-trimethoxystyryl)-2-methoxyphenyl 2-aminoacetate via Gabriel reaction

4.2.3.1 Synthesis of (Z)-5-(3,4,5-trimethoxystyryl)-2-methoxyphenyl 2-bromoacetate 6.

Combretastatin A-4 **1** (0.1 g, 0.32 mmol) was dissolved in dry CH_2Cl_2 (5 mL), 2-bromoacetic acid **5** (0.053 g, 0.38 mmol) was added followed by DCC (0.0783 g, 0.38 mmol) and DMAP (0.0193 g, 0.16 mmol). After stirring at room temperature overnight for 12 h under nitrogen, the DCU was filtered off and washed with small amounts of CH_2Cl_2 . Reaction mixture was extracted with 1 M NaHSO_4 (3 x 60 mL), 10 % Na_2CO_3 (3 x 60 mL) and then with brine (1 x 60 mL). Combined organic layers were dried over anhydrous Na_2SO_4 . The residue (0.137g, 0.30 mmol) was concentrated *in vacuo* to obtain **6** (0.137g, 93.7 percent yield). $^1\text{H-NMR}$ (400 MHz, δ , CDCl_3); 3.68 (6H, s), 3.79 (3H, s), 3.81 (3H, s), 4.02 (2H, s), 6.43 (2H, s), 6.47 (2H, s), 6.84 (1H, d, $J = 8$ Hz), 7.01 (1H, d, $J = 4$ Hz), 7.12 (1H, dd, $J = 4, 8$ Hz).

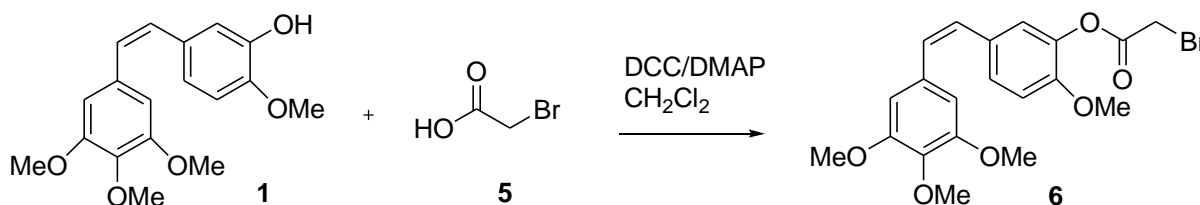


Figure 4.5 Synthesis of molecule 6

4.2.3.2. Synthesis of ((Z)-5-(3,4,5-trimethoxystyryl)-2-methoxyphenyl 2-(1,3-dioxisoindolin-2-yl)acetate 7. (Z)-5-(3,4,5-trimethoxystyryl)-2-methoxyphenyl-2-bromo

acetate **6** (0.250 g, 0.57 mmol) was dissolved in dry ACN (5 mL). Potassium phthalimide (0.16 g, 0.86 mmol) was added. It was stirred at room temperature for 1 h. Later, the solution was refluxed at 90 °C for another 1 hour. After the reaction completed, ACN was evaporated followed by dilution with CH₂Cl₂ (10 mL). The solution was washed with distilled H₂O (3 x 10 mL) and the organic layer was dried over anhydrous Na₂SO₄. The product was concentrated in *vacuo*. Crude was purified by column chromatography to obtain pure product (0.209 g, 73 percent yield). ¹H-NMR (400 MHz, δ, CDCl₃); 7.88 (2H, m), 7.74 (2H, m), 7.10 (1H, dd, *J* = 4, 8 Hz), 7.05 (1H, d, *J* = 4, Hz), 6.81 (1H, d, *J* = 8 Hz), 6.45 (2H, s), 6.43 (2H, s), 4.66 (2H, s), 3.81 (3H, s), 3.79 (3H, s), 3.65 (6H, s).

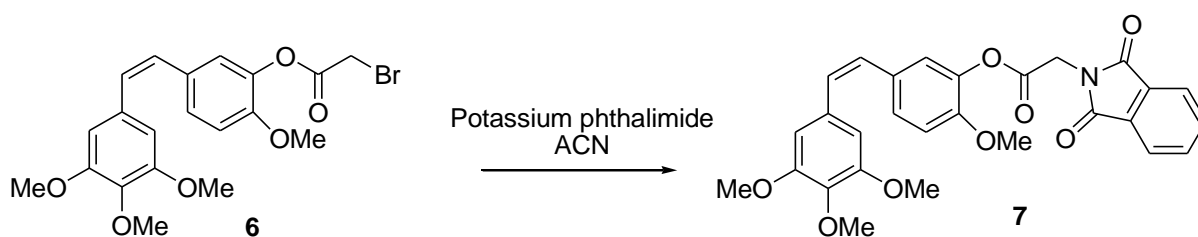


Figure 4.6 Synthesis of molecule **7**

4.2.3.3. Synthesis of ((Z)-5-(3,4,5-trimethoxystyryl)-2-methoxyphenyl 2-aminoacetate 4. ((Z)-5-(3,4,5-trimethoxystyryl)-2-methoxyphenyl 2-(1,3-dioxoisindolin-2-yl)acetate **7** (0.1 gr, 0.199 mmol) was dissolved in EtOH (5 mL) and CH₂Cl₂ (1 mL). Hydrazine hydrate (0.6 mL) was added and the solution was stirred at room temperature for 5 h. Later, it was concentrated and the product was purified by column chromatography.

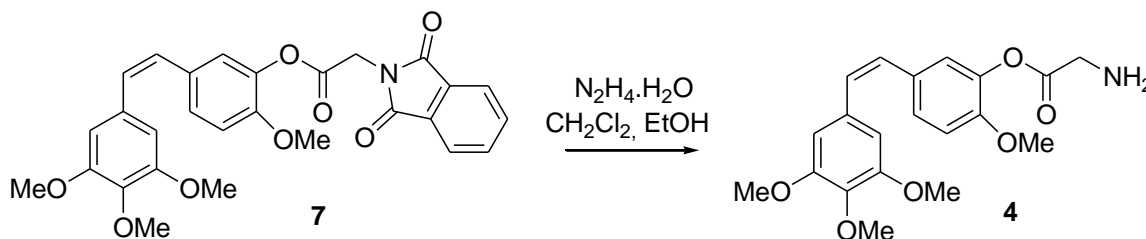


Figure 4.7 Gabriel Synthesis of molecule **4**

4.2.4. Synthesis of (Z)-5-(3,4,5-trimethoxystyryl)-2-methoxyphenyl 2-aminoacetate via Staudinger reaction

4.2.4.1. Synthesis of (Z)-5-(3,4,5-trimethoxystyryl)-2-methoxyphenyl 2-azidoacetate 8. To a solution of (Z)-5-(3,4,5-trimethoxystyryl)-2-methoxyphenyl 2-bromoacetate **6** (0.10 g, 0.229 mmol) was dissolved in THF (10 mL). To the solution, sodium azide was added (0.15 g, 2.29 mmol) and stirred at 55 °C for 12 h. After the reaction was completed, it was diluted with distilled water (10 mL) and hexane:EtOAc (20 mL, 50:50) was added. Organic phase was extracted with distilled water (3 x 20 mL), concentrated and was dried over anhydrous Na₂SO₄. The product was controlled characterized by IR spectrum. FTIR (cm⁻¹); 2107.4, 1772.5.

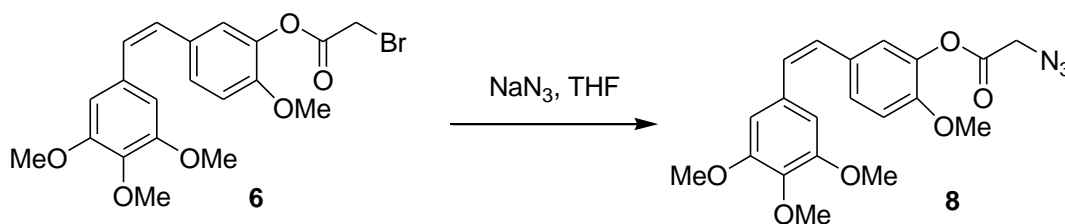


Figure 4.8 Synthesis of molecule **8**

4.2.4.2. Synthesis of (Z)-5-(3,4,5-trimethoxystyryl)-2-methoxyphenyl 2-aminoacetate 4. (Z)-5-(3,4,5-trimethoxystyryl)-2-methoxyphenyl 2-azidoacetate **8** (0.10 g, 0.25 mmol) was dissolved in THF (5 mL) under nitrogen. Triphenylphosphine (0.1 g, 0.375 mmol) was also dissolved in THF (5 mL) in another round bottom flask. Second solution was added (Z)-5-(3,4,5-trimethoxystyryl)-2-methoxyphenyl 2-azidoacetate solution slowly. Later, distilled water (50 μL) was injected to the mixture. Reaction was stirred for 2 h at room temperature. Later, it was diluted with EtOAc (10 mL) & water (10 mL) and the two phases were separated. Aqueous layer was extracted with EtOAc (3 x 10 mL). Combined organic phases were extracted with brine (3 x 10 mL) and dried over anhydrous Na₂SO₄. The solution was concentrated in *vacuo*.

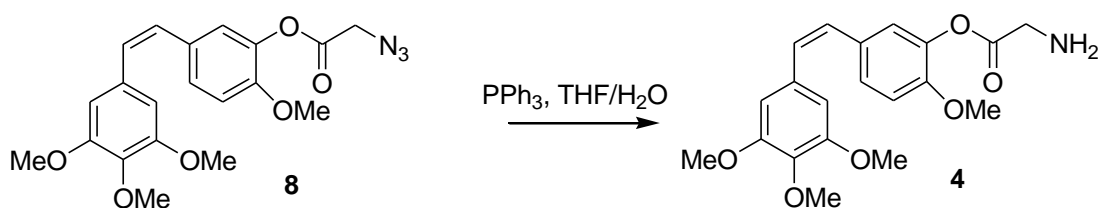


Figure 4.9 Synthesis of molecule 4

4.2.5. Synthesis of *Z*-5-(3,4,5-trimethoxystyryl)-2-methoxyphenyl 4-amino butanoate via Staudinger reaction

4.2.5.1 Synthesis of *(Z)*-5-(3,4,5-trimethoxystyryl)-2-methoxyphenyl 4-azidobutanoate 10.

Combretastatin A-4 **1** (0.1 g, 0.32 mmol) was dissolved in dry CH_2Cl_2 (5 mL), 4-azidobutanoic acid **9** (45 mg, 0.35 mmol) was added followed by DCC (0.0783 g, 0.38 mmol) and DMAP (0.0193 g, 0.16 mmol). After stirring at room temperature overnight under nitrogen, the DCU was filtered off and washed with small amounts of CH_2Cl_2 . Reaction mixture was extracted with 1 M NaHSO_4 (3 x 60 mL), 10 % Na_2CO_3 (3 x 60 mL) and then with brine (1 x 60 mL). Combined organic layers were dried over anhydrous Na_2SO_4 . The residue (0.137g, 94 percent yield) was concentrated in *vacuo*. ^1H NMR (CDCl_3 , δ , ppm); 7.10 (1H, dd, $J = 8.4, 2.1$ Hz), 6.98 (1H, d, $J = 2.1$ Hz), 6.83 (1H, d, $J = 8.4$ Hz), 6.48 (2H, s), 6.44 (2H, s), 3.82 (3H, s), 3.78 (3H, s), 3.69 (6H, s), 3.40 (2H, t, $J = 7.1$ Hz), 2.63 (2H, t, $J = 7.1$ Hz), 1.98 (2H, m). FTIR (cm^{-1}); 2095.80, 1760.45.

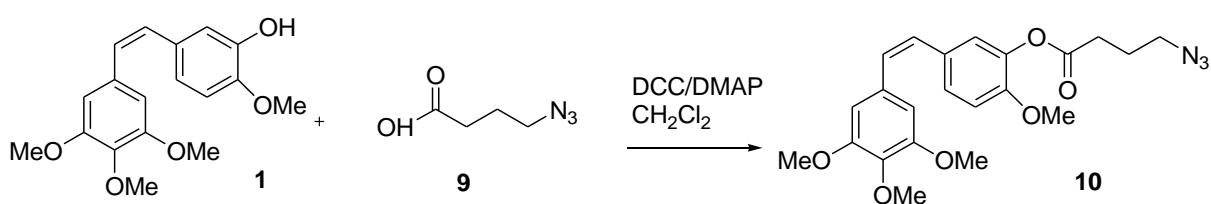


Figure 4.10 Synthesis of molecule 10

4.2.5.2. Synthesis of *(Z)*-5-(3,4,5-trimethoxystyryl)-2-methoxyphenyl 4-aminobutanoate 14.

(Z)-5-(3,4,5-trimethoxystyryl)-2-methoxyphenyl 4-azidobutanoate **10** (0.10 g, 0.25 mmol) was dissolved in THF (5 mL) under nitrogen. Triphenylphosphine (0.10 g, 0.375 mmol) was also dissolved in THF (5 mL) in another round bottom flask. Second solution was added *(Z)*-5-(3,4,5-trimethoxystyryl)-2-methoxyphenyl 4-azidobutanoate solution slowly. Later, distilled water (50 μL) was injected to the mixture. Reaction was stirred for 2 hours at room

temperature. Later, it was diluted with EtOAc (10 mL) & water (10 mL) and the two phases were separated. Aquous layer was extracted with EtOAc (3 x 10 mL). All organic phases were collected and extracted with brine (3 x 10 mL) and dried over anhydrous Na₂SO₄. The product was concentrated in *vacuo*.

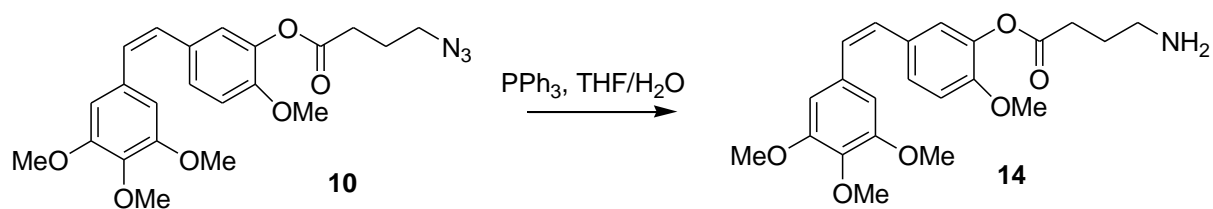


Figure 4.11 Synthesis of molecule **14**

APPENDIX

¹H NMR and IR data of the newly synthesized compounds are included.

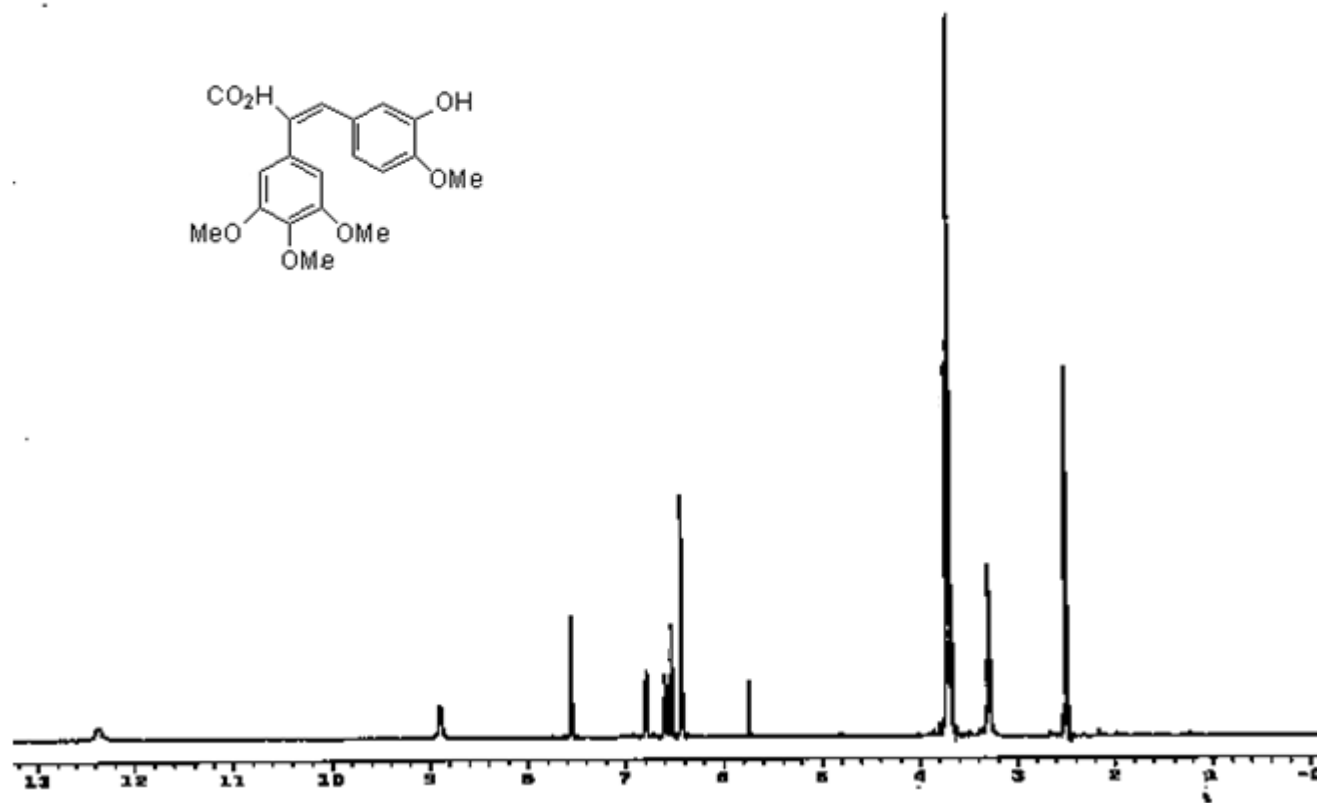


Figure A.1. ^1H NMR of propenoic acid **13**

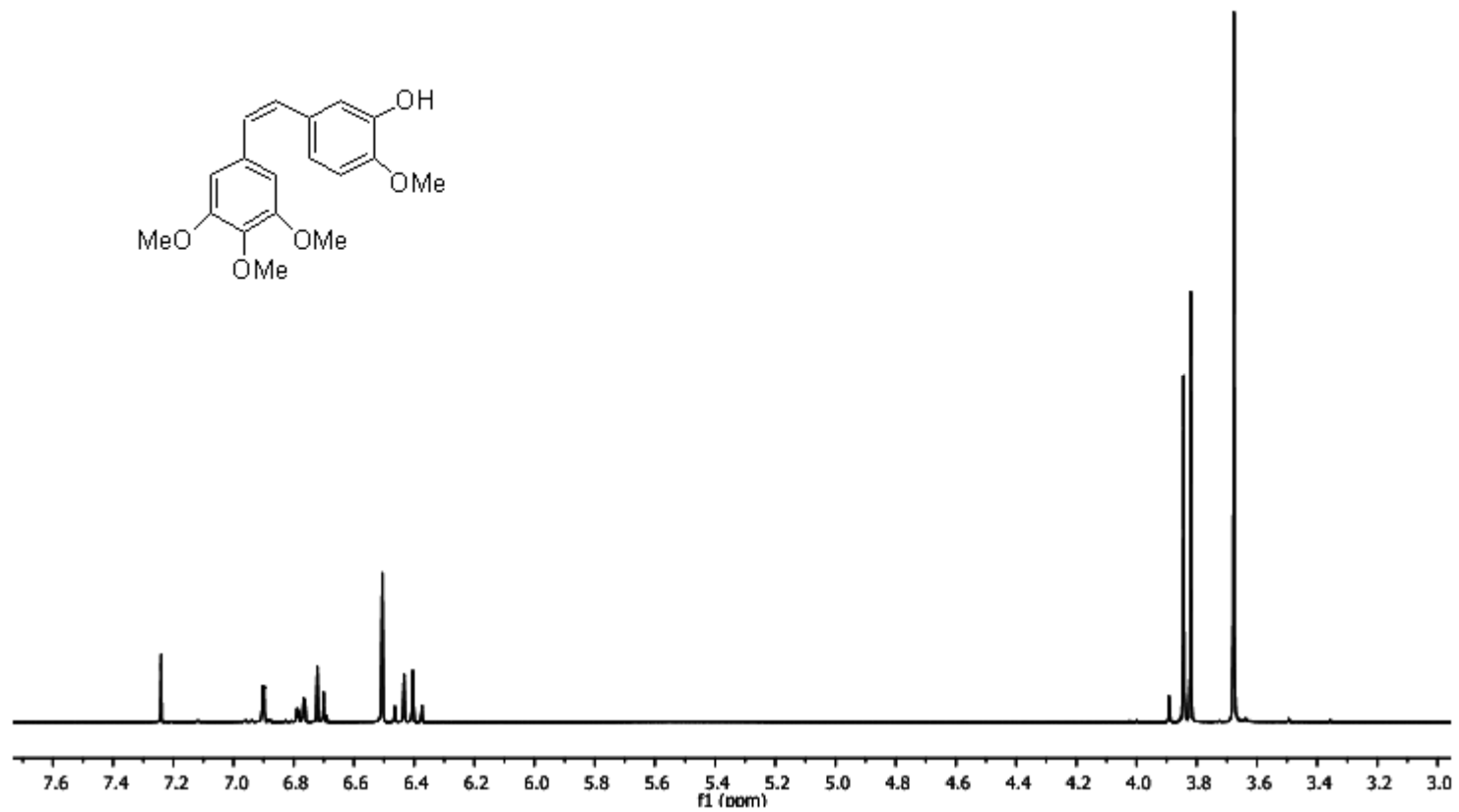


Figure A.2. ^1H NMR of CA-4 1

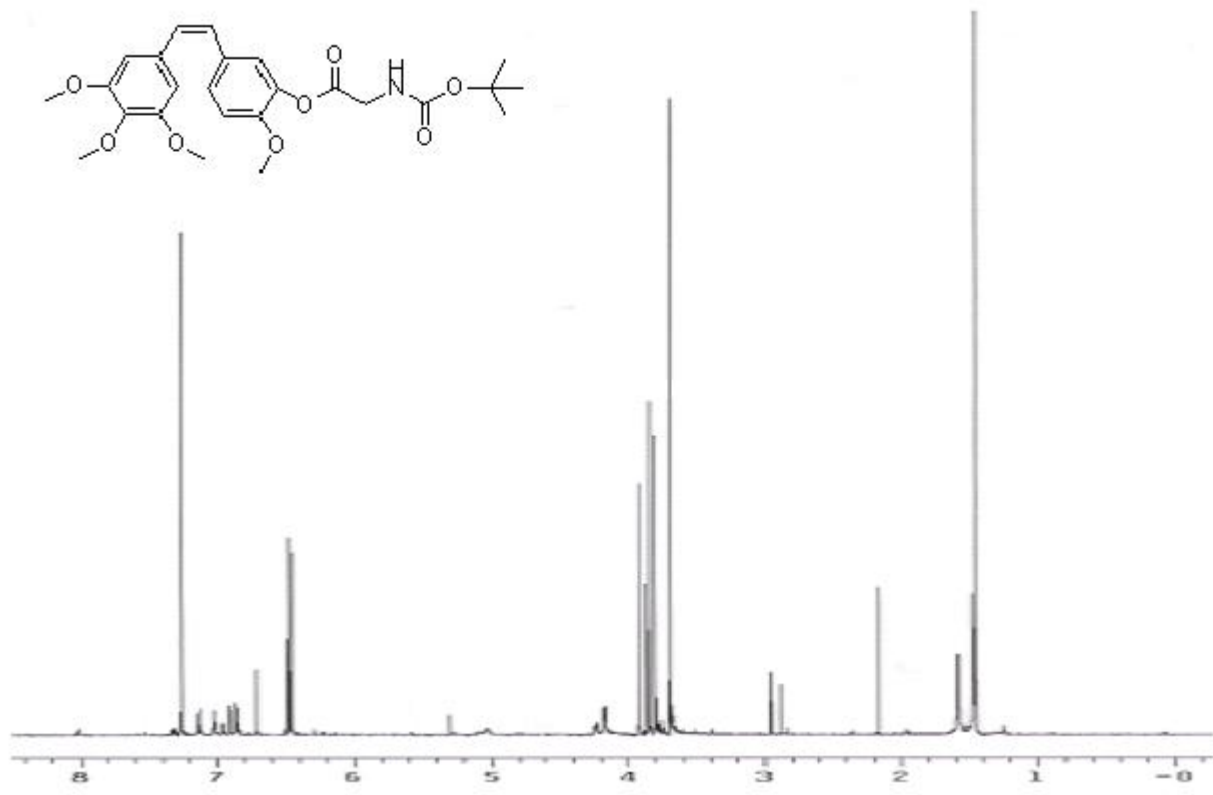


Figure A.3. ¹H NMR of the molecule 3

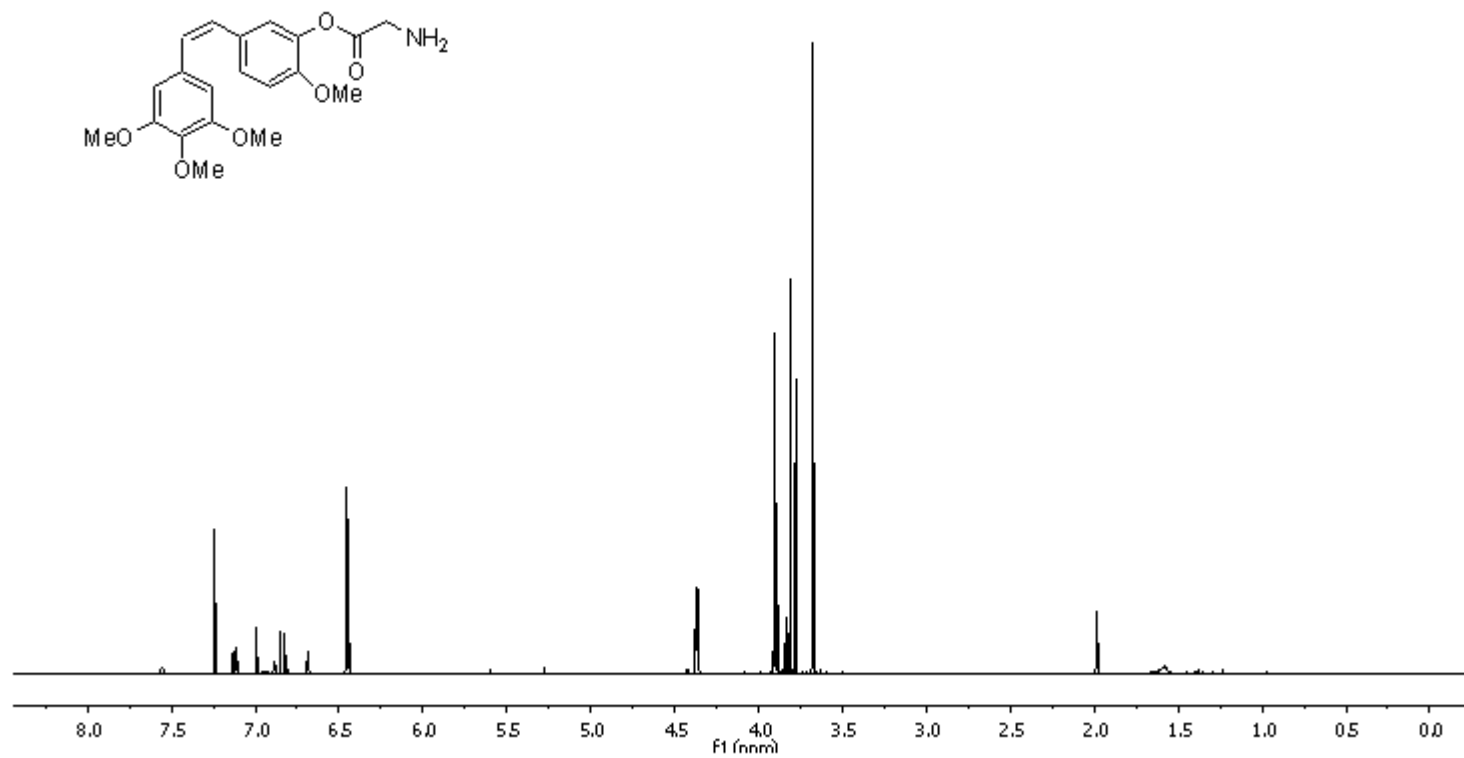


Figure A.4. ¹H NMR of the molecule 4

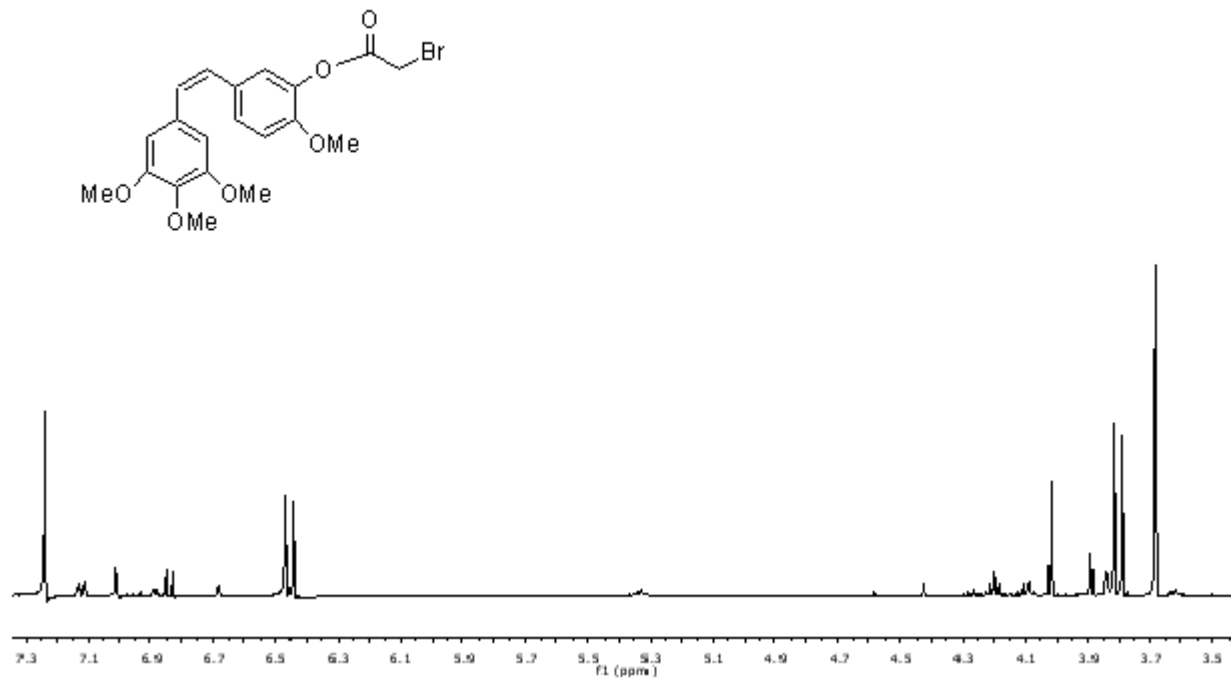


Figure A.4. ^1H NMR of the molecule **6**

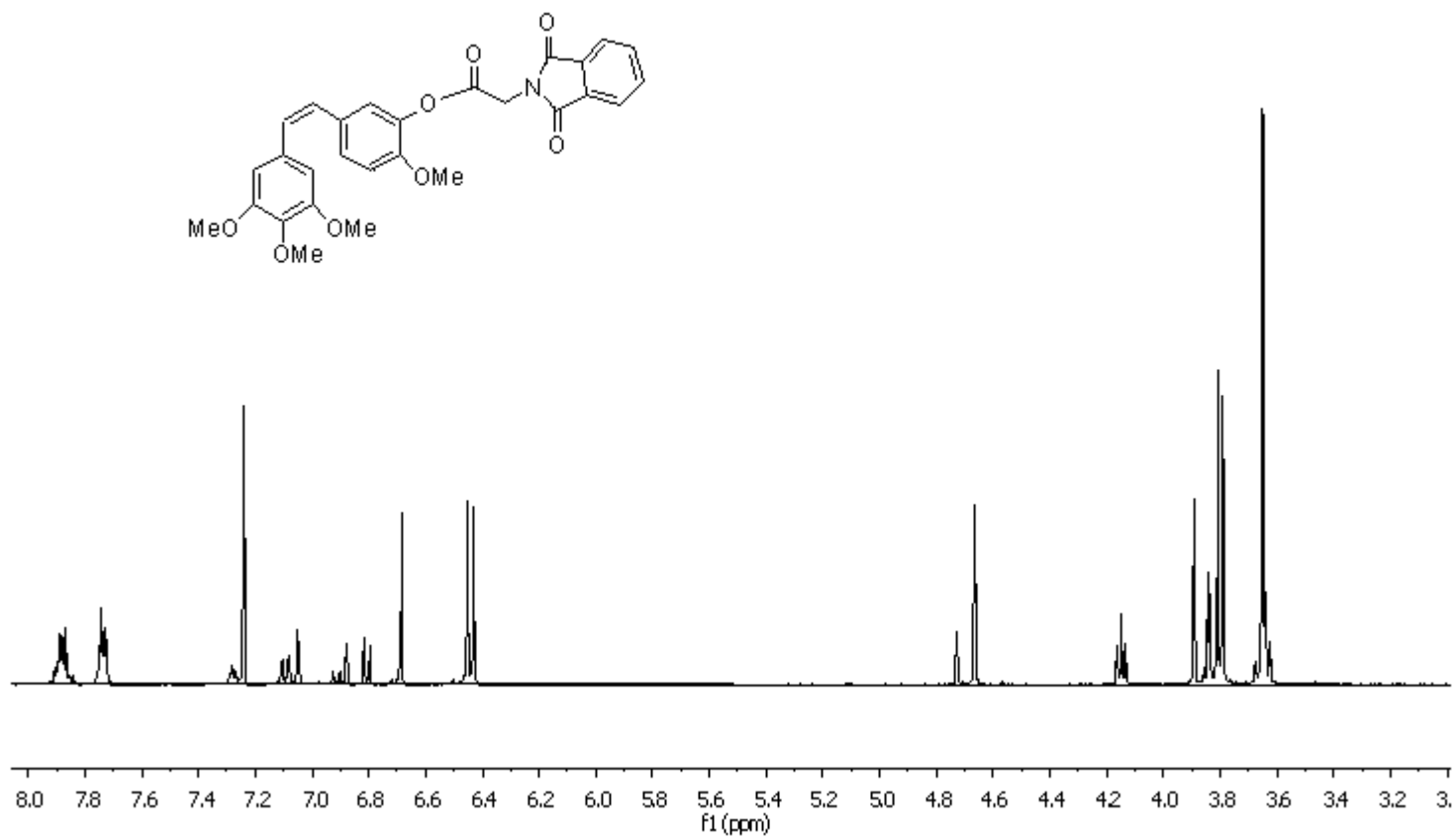


Figure A.5. ^1H NMR of the molecule 7

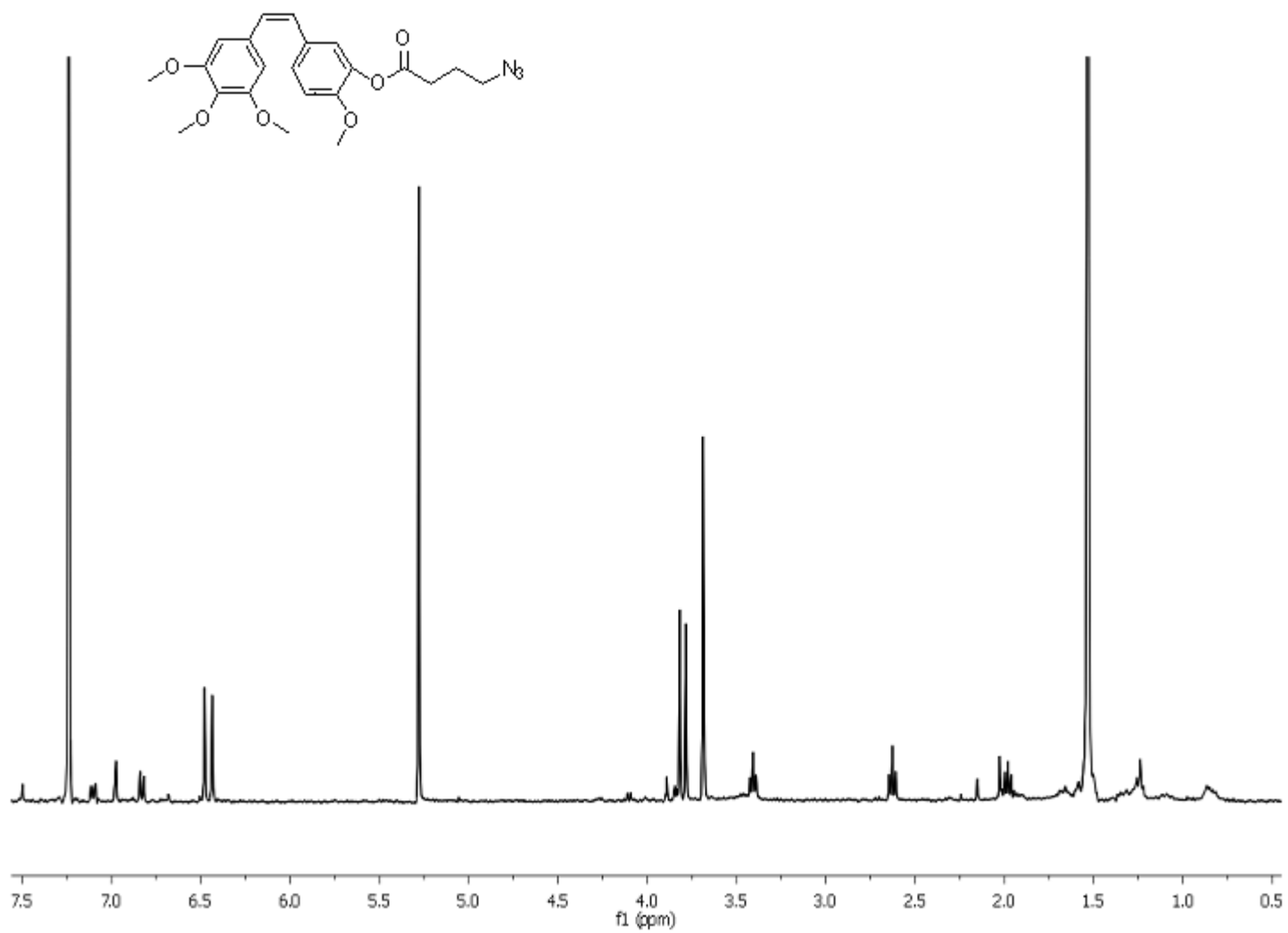


Figure A.6. ^1H NMR of the molecule **10**

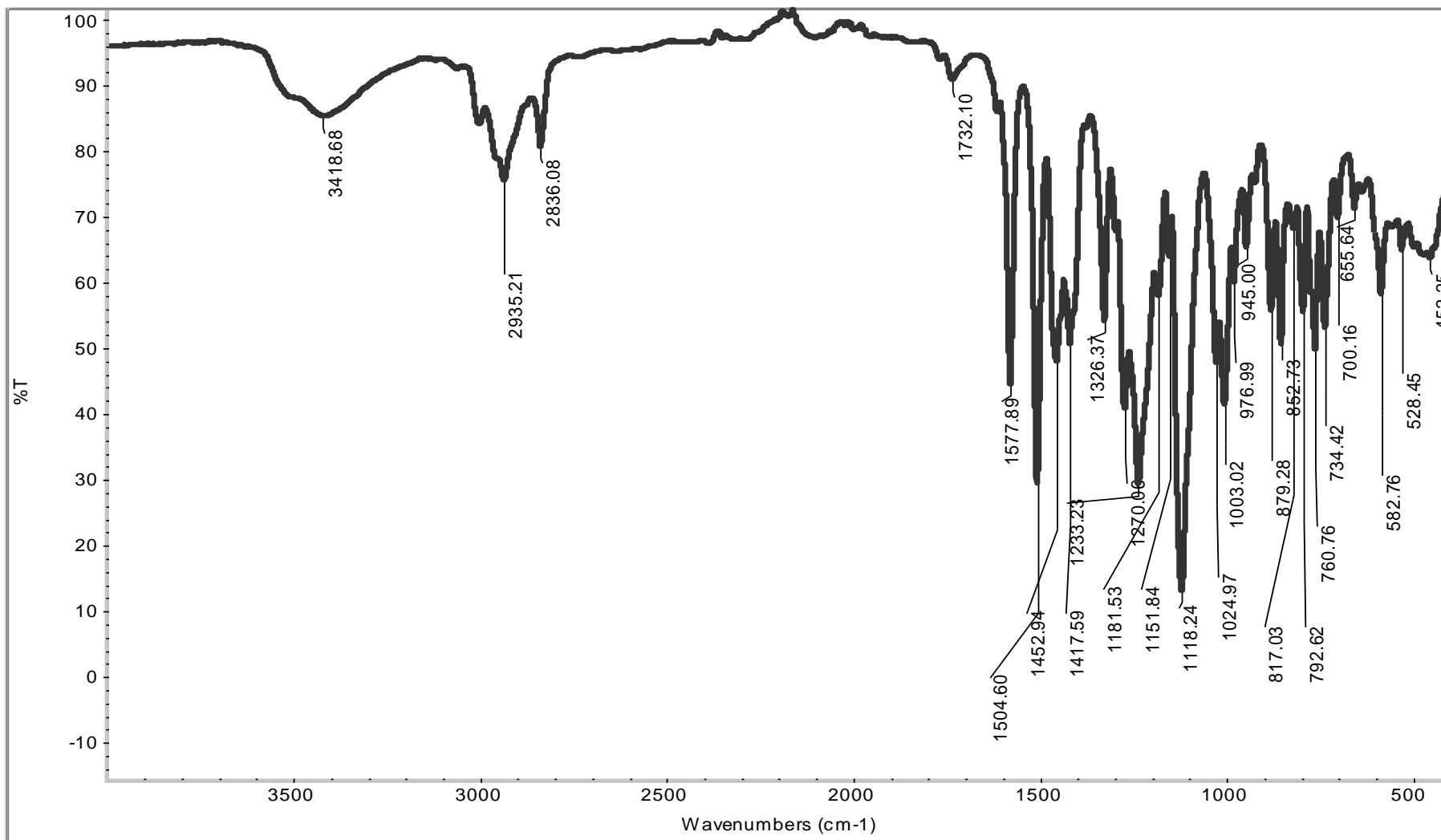


Figure A.8. IR spectrum CA-4 1

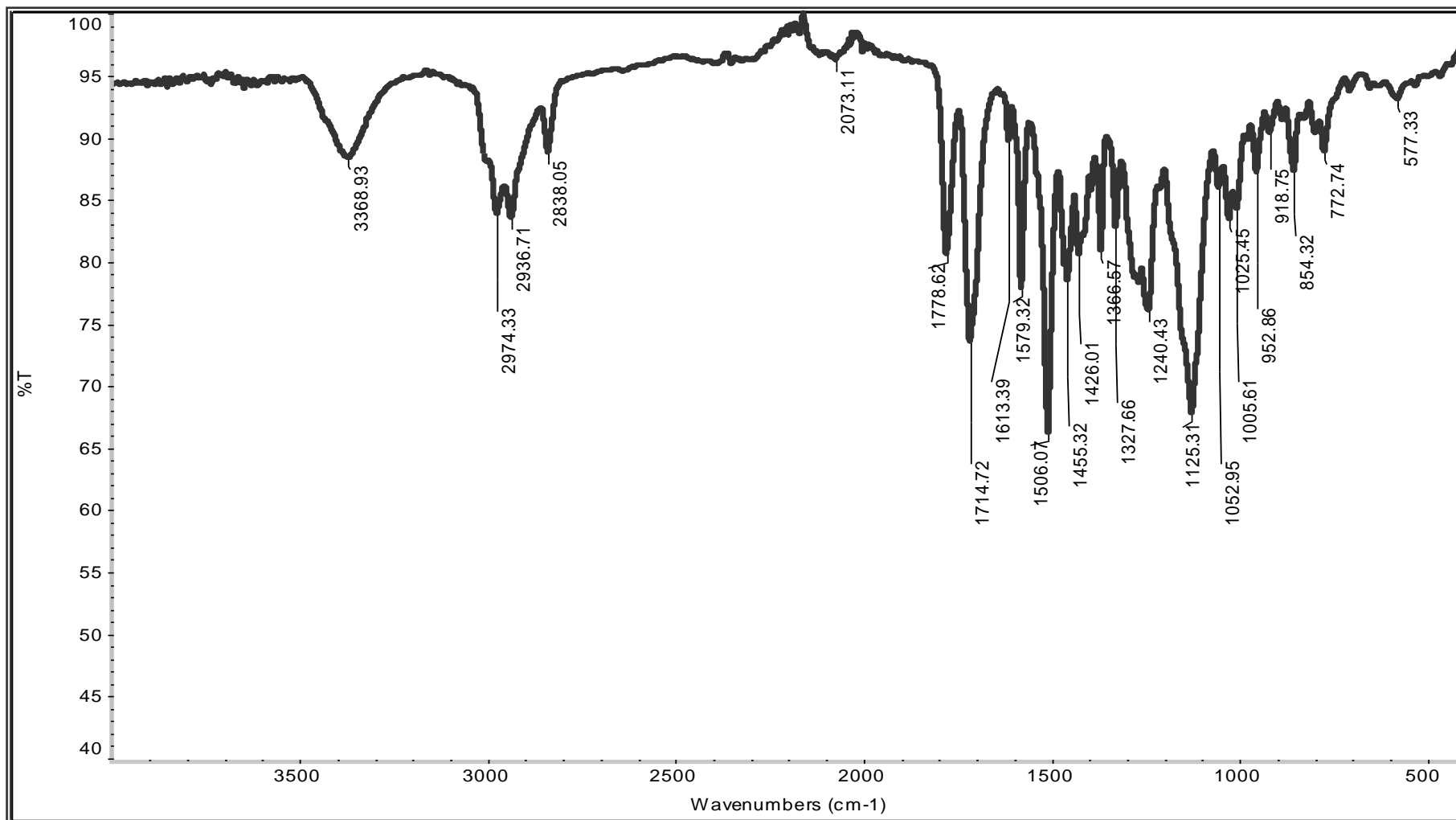


Figure A.9. IR spectrum of molecule 3

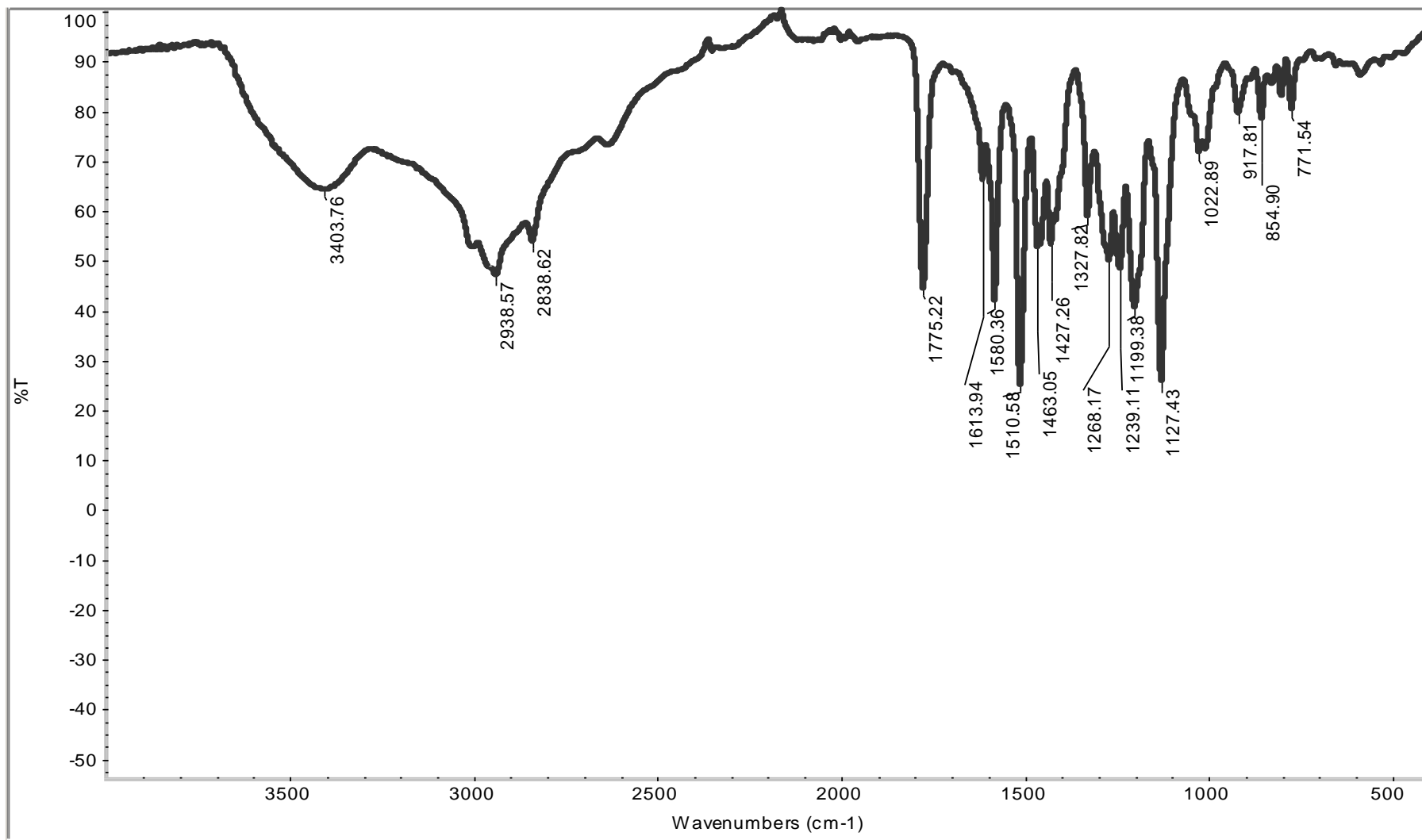


Figure A.10. IR spectrum of the molecule **4**

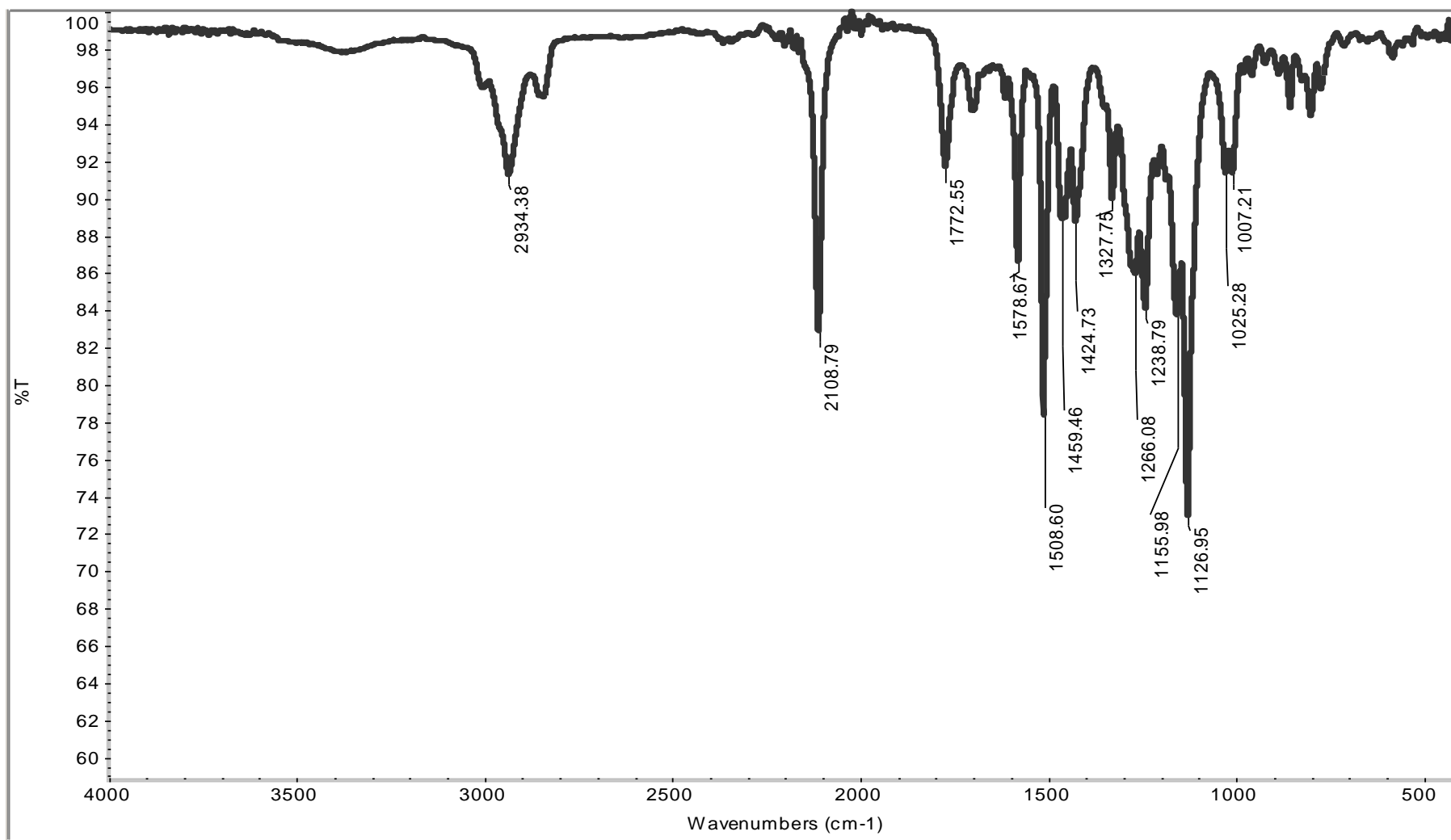


Figure A.11. IR spectrum of the molecule **8**

REFERENCES

1. Hanahan, D. and R. A. Weinberg, "The Hallmarks of Cancer", *Cell*, Vol. 100, pp. 57–70, 2000
2. Qiao, M. and A. B. Pardee, "Biomarkers, Receptors, and Pathways to Lethal Cancer", *Journal of Cellular Biochemistry*, Vol. 102, pp. 1076–1086, 2000
3. Biospace Lab, Molecular Imaging in Real Time for Life Sciences, http://www.biospacelab.com/html/Images/pi_ia7.gif, 2009
4. World Health Organization, Directing and Coordinating Authority for Health, <http://www.who.int/en/>, 2010
5. Jemal, A., Siegel, R., Ward, E., Hao, Y., Xu, J. and M. J. Thun, "Cancer Statistics", *A Cancer Journal for Clinicians*, Vol. 59, pp. 225-249, 2009.
6. Goody, R. B., Choong, E. S., Calderwood, J., Law, S. J. M., Mazdai, G., Hanna, G. G. and J. A. McAleer, "Mortality within 30 Days for Patients Older than 70 Years Receiving Chemotherapy: a Single-institution Retrospective Analysis", *Journal of Hong Kong College Radiol*, Vol. 12, pp. 95-102, 2010
7. Folkman, J., "Angiogenesis in Cancer, Vascular, Rheumatoid and Other Disease", *Nature Medicine*, Vol. 1, pp. 27-31, 1995
8. Lancrin, C., Sroczynska, P., Stephenson, C., Allen, T., Kouskoff, V. and G. Lacaud, "The Haemangioblast Generates Haematopoietic Cells Through a Haemogenic Endothelium Stage", *Nature*, Vol. 457, pp. 892-895, 2009
9. Carmeliet, P. and R. K. Jain, "Angiogenesis in cancer and other diseases", *Nature*, Vol. 407, pp. 249-257, 2000

10. Barresi, V., Vitarelli, E. and S. Cerasoli, "Semaphorin3A Immunohistochemical Expression in Human Meningiomas: Correlation with the Microvessel Density", *Virchows Archiv*, Vol. 454, pp. 563-571, 2009
11. Cébe-Suarez, S., Zehnder-Fjällman, A., and K. Ballmer-Hofer, "The Role of VEGF Receptors in Angiogenesis; Complex Partnerships", *Cellular and Molecular Life Sciences*, Vol. 63, pp. 601–615, 2006
12. Auerbach, R., Lewis, R., Shinnars, B., Kubai, L. and N. Akhtar, "Angiogenesis Assays", *Clinical Chemistry*, Vol. 49, pp. 32-40, 2003
13. Siemann, D. W., "Vascular Targeting Agents", *Horizons in Cancer Therapeutics: From Bench to Bedside*, Vol. 3, pp. 4-15, 2002
14. Sandra, Liekens, S., De Clercq, E. and J. Neyts, "Angiogenesis: Regulators and Clinical Applications", *Biochemical Pharmacology*, Vol. 61, pp. 253–270, 2001
15. Discovery Medicine, "Targeted Therapy-Avastin", <http://www.discoverymedicine.com/Benjamin-Yang/2009/06/17/drug-profile-avastin>, 2009
16. Avendaño, C., and J. C. Menéndez, , *Medicinal Chemistry of Anticancer Drugs*, Elsevier, Oxford, 2008
17. Drug Development Technology, "Aspects of Drug Development and Research Process", <http://www.drugdevelopmenttechnology.com>, 2010
18. Tron, G. C., Pirali, T., Sorba, G., Pagliai, F., Busacca, S., and A. A. Genazzani, "Medicinal Chemistry of Combretastatin A4: Present and Future Directions", *Journal of Medicinal Chemistry*, Vol. 49, pp. 3033-3044.

19. Bonezzi, K., Taraboletti, G., Borsotti, P., Bellina, F., Rossi, R. and R. Giavazzi “Vascular Disrupting Activity of Tubulin-Binding 1,5-Diaryl-1*H*-imidazoles”, *Journal of Medicinal Chemistry*, Vol. 52, pp. 7906-7910, 2009.
20. Iyer, S., Chaplin, D. J., Rosenthal, D. S., Boulares, A. M., Li, L. Y. and M. E. Smulson, “Induction of Apoptosis in Proliferating Human Endothelial Cells by the Tumor-Specific Anti-angiogenesis Agent Combretastatin A-4”, *Cancer Research*, Vol. 58, pp. 4510-4515, 1998
21. Tozer, G. M., Prise, V. E., Wilson, J., Locke, R. J., Vojnovic, B., Stratford, M. R. L., Dennis, M. F. and D. J. Chaplin, “Combretastatin A-4 Phosphate as a Tumor Vascular-Targeting Agent: Early Effects in Tumors and Normal Tissues”, *Cancer Research*, Vol. 59, pp.1626–1634, 1999.
22. Drug Researcher, News on Drug Discovery, <http://www.drugresearcher.com/Emerging-targets/Oxigene-s-Zybrestat-cuts-tumour-blood-flow>, 2007
23. Siemann, D. W. and W. V. Shi, “Dual Targeting of Tumor Vasculature: Combining Avastin and Vascular Disrupting Agents”, *Anticancer Research*, Vol. 28, pp. 2027-2031, 2008
24. Duncan, R., “The Dawning Era of Polymer Therapeutics”, *Nature Reviews Drug Discovery*, Vol. 2, pp. 347-360, 2003.
25. Vicent, M. J. and R. Duncan, “Polymer Conjugates: Nanosized Medicines for Treating Cancer”, *Trends in Biotechnology*, Vol. 24, pp. 39-47, 2006
26. Fox, M. E., Szoka, F. C. and J. M. J. Frechet, “Soluble Polymer Carriers for the Treatment of Cancer: The Importance of Molecular Architecture”, *Accounts of Chemical Research*, Vol. 42, pp. 1141-1151, 2009.

27. Duncan, R., "Development of HPMA Copolymer-Anticancer Conjugates: Clinical Experience and Lessons Learnt", *Advanced Drug Delivery Reviews*, Vol. 61, pp. 1131–1148, 2009.
28. Singer, J. W., "Paclitaxel poliglumex (XYOTAX (TM), CT-2103): A macromolecular taxane", *Journal of Controlled Release*, Vol. 109, pp. 120–126, 2005.
29. Gaukroger, K., Hadfield, J. A., Hepworth, L.A., Lawrence, N. J. and A. T. McGown, "Novel syntheses of cis and trans isomers of combretastatin A-4", *J. Org. Chem.* Vol. 66, pp. 8135-8138, 2001